Artif Intell Rev (2018) 50:497–537
https://doi.org/10.1007/s10462-017-9550-x

# Review of liver segmentation and computer assisted detection/diagnosis methods in computed tomography

**Mehrdad Moghbel**[1] · **Syamsiah Mashohor**[1] · **Rozi Mahmud**[2] · **M. Iqbal Bin Saripan**[1]

Published online: 20 March 2017


**Abstract** Computed tomography (CT) imaging remains the most utilized modality for liver-related cancer screening and treatment monitoring purposes. Liver, liver tumor and liver vasculature segmentation from CT data is a prerequisite for treatment planning and computer assisted detection/diagnosis systems. In this paper, we present a survey on liver, liver tumor and liver vasculature segmentation methods that are using CT images, recent methods presented in the literature are viewed and discussed along with positives, negatives and statistical performance of these methods. Liver computer assisted detection/diagnosis systems will also be discussed along with their limitations and possible ways of improvement. In this paper, we concluded that although there is still room for improvement, automatic liver segmentation methods have become comparable to human segmentation. However, the performance of liver tumor segmentation methods can be considered lower than expected in both automatic and semi-automatic methods. Furthermore, it can be seen that most computer assisted detection/diagnosis systems require manual segmentation of liver and liver tumors, limiting clinical applicability of these systems. Liver, liver tumor and liver vasculature segmentation is still an open problem since various weaknesses and drawbacks of these methods can still be addressed and improved especially in tumor and vasculature segmentation along with computer assisted detection/diagnosis systems.

**Keywords** Image segmentation · Computer assisted detection/diagnosis · Liver tumor segmentation · Liver segmentation · Liver vasculature segmentation · Computed tomography

✉ Mehrdad Moghbel
mehrdad2275@gmail.com

[1] Department of Computer and Communication Systems, Faculty of Engineering, University Putra Malaysia, 43400 Serdang, Selangor, Malaysia

[2] Cancer Resource and Education Center, University Putra Malaysia, 43400 Serdang, Selangor, Malaysia

## 1 Introduction

Liver and liver tumor segmentation is a prerequisite for many clinical applications such as computer assisted detection/diagnosis (CAD), liver surgery planning, treatment planning and post-treatment evaluation. Apart from liver surgery planning, high accuracy for liver and liver tumor volume determination is also essential for Selective Internal Radiation Therapy (SIRT) planning and reducing the risk of excess or insufficient radiation dose as patient's liver volume determines the amount of radiation to be delivered. Manual delineation of these tumors are both time-consuming and the segmentation is reliant on the operator, for these reasons automatic segmentation of liver and liver tumors has been of interest for many researchers. The need for a proper segmentation is further underlined by the fact that liver cancer is amongst top cancers with the most fatalities while metastatic tumors are commonly originate from inside of the liver (Grendell et al. 1996; Habib et al. 2003). The purpose of this paper is to acquaintance the reader with the current state of the art methods, making a comparison between different methods easier. Furthermore, different performance evaluation metrics are discussed along with currently available public datasets.

Currently, the most commonly used approach for liver disease monitoring and evaluation is the contrast-enhanced computed tomography preceded by an initial ultrasound imaging (Hann et al. 2000). Over the past decade, several automatic and semi-automatic liver and liver tumor segmentation methods along with many CAD systems have been proposed by many researchers. In most of these studies, prior information like spatial location and shape of the liver are incorporated into segmentation process in order to cope with associated segmentation challenges. Also, several pre/post-processing steps are included to assist or refine the segmentation. Among all, most prominent and promising methods are mainly based on statistical shape models (SSMs), deformable models, probabilistic atlases, level sets, region growing, graph cuts, neural networks, rule-based systems, voxel classification and different clustering methods. However, most of the proposed CAD systems are based on manual segmentation of liver and liver tumors, making the clinical value of these CAD systems limited as manual liver and tumor segmentation by a radiologist can take up to two hours for a series. In the following sections, we review these methods and discuss their performance.

## 2 Classification of image segmentation techniques

All segmentation methods can be classified based on the amount of shape information used by the method (Erdt et al. 2012). With incorporating more shape information, an algorithm becomes more specialized. For example, a simple threshold based method can be used to segment any shape with similar properties (i.e. intensity). In contrast, a deformable model based segmentation optimized for livers will function poorly if applied to other organs such as spleen or kidneys. Simpler methods (i.e. thresholding) have the broadest application area concerning shape generalizability. Usually, these methods can be adjusted using a few parameters as they do not utilize a high degree of domain specific knowledge. For these methods, it might be enough to examine some cases representative of overall segmentation requirements or to consult a domain expert. On the other hand, more complex methods (i.e. deformable models) can be considered as highly specialized, as they are often only suitable for a particular segmentation scenario and have a high number of adjustable parameters as they utilize a high degree of domain specific knowledge. The number of adjustable

parameters in a segmentation method increases with the amount of shape domain knowledge utilized.

Nowadays, machine learning algorithms such as different clustering methods and support vector machines are increasingly being used as supportive tools to automate the segmentation methods and to support and enhance other segmentation methods by performing statistical analysis on a set of data originally generated by other segmentation algorithms. Therefore, machine learning concepts can be coupled with and used to enhance any existing segmentation algorithm. Complex segmentation problems are often modeled using a whole pipeline of different segmentation methods belonging to different classification concepts. In such a case, the method is classified based on the algorithm using the most domain specific knowledge, an approach using thresholding for initial segmentation and a model based method for refining this initial segmentation is considered as a model based method.

## 3 Medical value of segmentation

A main constraint for the surgical resection planning is the liver/tumor ratio after surgical resection (Nordlinger et al. 1996; Jagannath et al. 1986), known as the tumor burden. Tumor burden is also important as it can provide an accurate estimation of effectiveness of different treatment protocols and increase the treatment effectiveness by enabling the patient and the physician to select the best course of treatment (Gobbi et al. 2004; Bauknecht et al. 2010; Bolte et al. 2007; Bornemann et al. 2007; Fabel et al. 2011; Heussel et al. 2007; Kuhnigk et al. 2006; Puesken et al. 2010). Increasingly, the effectiveness of cytotoxic anti-cancer drugs is also evaluated using tumor burden analysis (Prasad et al. 2002; Heckel et al. 2014).

Liver and tumors segmentation allows easier computation of tumor burden, simplifying the surgical liver resection planning. Segmentation also provides a precise volume and location of the liver and any tumors inside the anatomical segments of the liver, simplifying the diagnosis. In addition, liver and tumor segmentation is also a prerequisite for many treatment options such as thermal percutaneous ablation (Rossi et al. 1996), percutaneous ethanol injection (Livraghi et al. 1995), radiotherapy surgical resection (Albain et al. 2009) and arterial embolization (Yamada et al. 1983). Furthermore, in treatments such as selective internal radiation therapy (Al-Nahhas et al. 2006), fractional dose calculation depend on the volume of the liver and tumors. Percutaneous thermal ablation treatments such as radiofrequency thermal ablation (Rossi et al. 1994) and microwave ablation (Liang et al. 2009) are other treatment options that can benefit from segmentation. Moreover, transarterial embolization and transcatheter arterial chemoembolization (Camma et al. 2002) can also benefit from this segmentation.

## 4 Publicly available datasets

Currently available public datasets include cancer imaging archive of the Frederick National Laboratory for Cancer Research (CIR dataset 2016), 3Dircadb dataset from Research Institute against Digestive Cancer (IRCAD) (IRCAD dataset 2016), The MIDAS liver tumor dataset from National Library of Medicines Imaging Methods Assessment and Reporting (IMAR) project (MIDAS dataset 2016) and Sliver'07 dataset from The Medical Image Computing and Computer Assisted Intervention Society MICCAI liver segmentation challenge (Sliver07 dataset 2016). Radiological experts manually outlined liver (Sliver'07, 3Dircadb),

liver tumor contours (MIDAS, 3Dircadb) and liver blood vessel contours (3Dircadb) for all images on a slice-by-slice basis in order to determine the ground truth while the cancer imaging archive dataset contains no expert segmentation. The number of slices in each series, the slice thickness and the pixel spacing varied from 64 to 502, 0.5 to 5.0 and 0.54 to 0.87 mm respectively. Most of the cases are pathologic involving metastasis cysts and tumors of different sizes and the image resolution is $512 \times 512$ in all cases. 3Dircadb and Sliver'07 datasets are segmented by a single radiologist while the MIDAS dataset has segmentation from five different radiologists.

## 5 Statistical performance evaluation metrics

### 5.1 Evaluating performance of segmentation methods

A brief introduction on six statistical performance measures commonly utilized in liver related segmentation methods is given below. Apart from the dice similarity coefficient, all other measures are suggested as a result of extensive review of possible validation metrics for liver and liver tumor segmentation from CT images by the MICCAI and were used by them in various challenges. However, majority of the methods in the literature (especially newer publications) mostly report their volumetric overlap error, relative volume difference and dice similarity coefficient. Furthermore, most distance based measures common in evaluating accuracy of segmentation methods were dropped from the evaluation criterions commonly used in medical imaging by a study that described best and most common performance measures currently being reported in the literature (Taha and Hanbury 2015).

### 5.2 Volumetric overlap error

Volumetric overlap error (VOE) expressed in percent, represents the number of pixels in the intersection of segmented region (A) and the ground truth (B), divided by the number of pixels in the union of A and B (Heimann et al. 2009). This value is 0 for a perfect segmentation while any increase in this value correlates to increased discrepancy between segmentation and ground truth with 100 as the lowest possible value, when there is no overlap at all between segmentation and reference. It can be calculated in percent from the following formula:

$$\mathrm{VOE} = ((|\mathrm{A} \cap \mathrm{B}| \,/\, |\mathrm{A} \cup \mathrm{B}|) - 1) \times 100 \tag{1}$$

### 5.3 Dice similarity coefficient

Dice similarity coefficient (DSC) also represents the overall performance of the algorithm in correctly including the pixels of the ROI inside the segmentation. It can be calculated by the following formula:

$$\mathrm{DSC} = 2\,|\mathrm{A} \cap \mathrm{B}| \,/\, (|\mathrm{A}| + |\mathrm{B}|) \tag{2}$$

A value of 0 represents no overlap between the segmented region and ground truth while a value of 1 represents perfect segmentation. Note that the Jaccard (JAC) index is usually excluded in cases where DSC is reported because it provides the same ranking as:

$$\mathrm{JAC} = \mathrm{DSC}/2 - \mathrm{DSC} \tag{3}$$

### 5.4 Relative volume difference

Relative volume difference (RVD) expressed in percent (Heimann et al. 2009), whereby the total volume of the segmented region is divided by the total volume of ground truth. It can be calculated by the following formula:

$$\text{RVD} = ((\text{total volume of segmented region}/\text{total volume of ground truth}) - 1) \times 100 \quad (4)$$

This measure should not be utilized solely to assess the performance of any segmentation method as a value of 0 (no volume difference) can also be obtained from an inaccurate segmentation, as long as the segmented region volume is equal to the volume of the ground truth. Please note that negative values represent under segmentation while positive values point to over segmentation.

### 5.5 Average symmetric surface distance

Average symmetric surface distance (ASD), in millimeters, is another measure for evaluating the segmentation performance (Heimann et al. 2009). First, the voxels in the border of the reference and the segmentation and are identified. For each voxel along segmentation border, the closest voxel along the reference border is determined (using Euclidean distance, not signed distances, so taking into account the different resolutions in the different scan directions). The average of all these distances gives the average symmetric absolute surface distance. A value of 0 (mm) represents perfect segmentation.

### 5.6 Root mean square symmetric surface distance

Root mean square symmetric surface distance (RMSD), in millimeters, is similar to the average symmetric surface distance measure, but the root value of the squared average symmetric surface distance distances between the two sets of border voxels is computed (Heimann et al. 2009). A value of 0 (mm) represents perfect segmentation.

### 5.7 Maximum symmetric surface distance

Maximum symmetric surface distance (MSD), in millimeters, is similar to the average symmetric surface distance measure but in this case, the maximum of all voxel distances is taken instead of the average (Heimann et al. 2009). A value of 0 (mm) represents perfect segmentation. However, this measure is not that popular for representing the segmentation performance as a single misplaced pixel on the segmentation can result in a large maximum symmetric surface distance without being that informative of overall segmentation performance.

### 5.8 Accuracy of a CAD system

Definitions of True and False positive/negative

- True positive: Sick people correctly diagnosed as sick (TP)
- False positive: Healthy people incorrectly identified as sick (FP)
- True negative: Healthy people correctly identified as healthy (TN)
- False negative: Sick people incorrectly identified as healthy (FN)

Classification accuracy shows the performance of a CAD system is correctly classifying any given particular class calculated by the following formula:

$$\text{Accuracy} = \frac{\text{number of TP} + \text{number of TN}}{\text{number of TP} + \text{number of FP} + \text{number of TN} + \text{number of FN}} \quad (5)$$

## 6 Liver segmentation

Despite lots of attention, fully automatic liver and liver tumor segmentation from a CT volume remains a challenging task, mainly because of the variability of the liver and tumor shapes and the intensity patterns inside and in the neighborhood of them. Being a soft organ, the liver shape is highly dependent on adjacent organs within the abdomen. Moreover, many pathologies can have a strong effect on the appearance and the shape of the liver while most of the time clearly defined edges are not visible on many sides of the liver. In particular, the intensity differences between the liver and the heart or the spleen or the stomach are very small as illustrated in Fig. 1. Due to similar intensities between adjacent organs, tissues and vague boundaries, low-level image processing algorithms are not sufficient for liver segmentation. Moreover, CT images are usually acquired using an injection protocol in order to enhance tumors. However, this enhancement changes with the injection phase and then the enhancement increases the noise inside the images that are already very noisy for the liver without any enhancement.

In order to cope with above problems encountered, most of the liver segmentation methods utilize prior information such as intensity distributions inside liver, shape or location of liver. Explicit and implicit SSMs tries to statistically model the complex shape of liver. However, as pointed in, even with a large number of training samples, structure of liver cannot be captured completely thus SSM based methods are generally combined with an additional energy based free deformation step.

Another way of incorporating prior shape information is the use of probabilistic atlases (PA) since they provide both prior shape and spatial information. However, these methods suffer from misrecognition of surrounding tissues which is the primary source of error for PA based methods. Accurate modeling of intensity distributions inside the liver provides another prior information about liver. However, inhomogeneous intensity value appearances inside liver make distribution estimation process difficult especially in pathological livers.


**(a)** **(b)** **(c)**

**Fig. 1** Examples of difficulties of liver segmentation: sample CT slices with ambiguous boundary between liver and heart (**a**), stomach (**b**) and tumor must be included in segmentation (**c**)

To address above issues, a challenge was presented to different researchers by the Medical Image Computing and Computer-Assisted Intervention Society (MICCAI) to segment liver on clinical bases known as Sliver'07 liver segmentation challenge (Heimann et al. 2009). From this challenge and consequent publications, it can be observed that many approaches have been developed and considered for segmentation of the liver envelope. These methods are discussed in detail in the following sections.

### 6.1 Statistical shape models and deformable model based methods

Introduced by Cootes et al. (1995), statistical shape models have become a popular choice for segmenting medical images. They utilize prior information by providing global shape constraints based on a training set and usually have robust performances. However, SSMs constraint the segmentation in the space of shapes learned from training data thus requiring a large training dataset. Although SSMs are robust, they often lack the flexibility to accurately adapt to a structure with high variations in shape such as pathological livers. Thus, many proposed SSMs are followed by a free form deformation step utilizing deformable models (Heimann et al. 2006, 2007a, b; Kainmüller et al. 2007; Zhang et al. 2010; Erdt et al. 2010; Wang et al. 2015b).

As an alternative, construction of local shape models has been proposed as a way of accomplishing flexibility in SSMs (Okada et al. 2008a, b). Different initializations, shape correspondences, appearance models and search algorithms have been utilized by SSMs used for liver segmentation. However, the contribution of SSM remains significant as a recent SSM with a subsequent free deformation step offered one of the best results for automatic liver segmentation (Tomoshige et al. 2014). Montagnat and Delingette (1997) proposed a 2-simplex mesh based deformable model where vertices of the mesh experience both local forces from curvature and gradient information along with the global force from shape constraint and transformation (i.e. rigid, affine, cubic b-spline). For initialization, a template liver shape is selected and its location is determined by using iterative closest point algorithm between the template and coarsely segmented liver. Lamecker et al. (2004) proposed an automatic 3D-SSM of liver based on an appearance model, modeled on intensity profiles along the liver boundary. A voxel can be labeled as 'inside', 'outside' or 'no decision' in the boundary search step followed by a weighted least squares estimation to obtain new shape parameters. In order to achieve robustness, in this implementation, the voxels labeled as 'no decision' receive a weight of zero. Although this method is automatic, a semi-automatic mapping procedure was utilized for building the model where corresponding points on the liver are marked by a user.

Saddi et al. (2007) proposed an automatic liver SSM with deformable models based on non-rigid template matching. A binary template is aligned to an image by maximizing the intensity distribution of voxels inside and outside of the liver. Initialization is achieved by aligning the center of gravities of template and image. Initial segmentation is done by finding the boundary minimizing the segmentation energy with a gradient descent algorithm followed by a non-rigid registration for a refined segmentation. Heimann et al. (2007b) proposed a hybrid method utilizing evolutionary algorithm, SSM and a deformable mesh. Initialization of SSMs is achieved by a multi-resolution approach utilizing an evolutionary algorithm. In this implementation, a population containing shapes is obtained by randomly selecting transformation and parameters of SSM. Afterwards, all population members are evaluated using local appearance model based on k-nearest neighbor (kNN) classifier utilizing profile probabilities proposed by Van Ginneken et al. (2002). After initialization, a deformable mesh is fitted based on internal forces keeping the mesh close to underlying SSM and external forces expanding

the mesh towards best-fit data selected via graph-based optimal surface detection algorithm (Li et al. 2006a). Saito et al. (2016) proposed an automatic liver segmentation algorithm utilizing statistical shape models (SSM) where SSM-guided expectation–maximization (EM) algorithm without using spatial standardization for better handling of pathological livers. The segmentation is then refined utilizing a graph cut based approach.

Kainmüller et al. (2007) proposed an automatic SSM based on heuristic intensity model with a deformable mesh for a refined segmentation. The model included shapes built from 112 livers with the proposed SSM containing almost 7000 landmark points. Three vector fields with one utilizing heuristic appearance model, the second one drawing each vertex towards the center of its direct neighbors and the last one to ensure the mesh does not leave a narrow band defined around the SSM segmentation are utilized for guiding the mesh evolution. Although this method is automatic, a semi-automatic mapping procedure was utilized for building the model where principal liver edges are marked by a user. The segmentation is based on the identification of the right lung lobe (as liver sits just below the lung lobe) by thresholding and morphological operations followed by initial segmentation of the liver. Afterwards, freely deformable mesh is utilized to get a refined segmentation.

Seghers et al. (2007) proposed to employ local information for solving the flexibility problem of SSM. Unlike the global shape models, in this implementation, a statistical model for each edge of the mesh is utilized for capturing mean and covariance of the edge vector. Ling et al. (2008) proposed a hierarchical SSM, dividing the mesh into patches for the construction of a local shape model. In every hierarchy level, both image and landmark points of SSMs are down sampled and SSM is constructed using down-sampled mesh. Initialization is achieved using a learning based boundary search where pose parameters and some of SSM parameters are found by utilizing marginal space learning (Zheng et al. 2007). Zhang et al. (2010) proposed an SSM employing an optimal surface detection strategy. First, a rough initialization is obtained through generalized Hough transform, then the intensity at the current landmark and gradient information are used to search for candidate points. An optimal surface detection algorithm based on graph theory (Li et al. 2006a) is utilized for the relaxation step. Erdt et al. (2010) proposed an SSM method combining learned local constraints with constraints directly obtained from current curvature for coping with the drawback of SSM in regions with high curvature.

### 6.2 Probabilistic atlas based methods

Probabilistic atlases utilize both the prior shape and the spatial location information to achieve a refined segmentation. Furthermore, relations between adjacent structures can be effectively modeled utilizing multi-class atlases. On general, the procedure for computing PA starts with registering all the training set images onto a pre-selected image. Afterwards, manual delineations are warped onto the template label image and averaged to provide a PA. Atlas based segmentation methods can be separated by their computation of PA and the way it is incorporated into the segmentation.

Park et al. (2003) proposed the first PA for abdominal organs. In this implementation, a PA for abdomen consisting of liver, kidneys and spinal cord is constructed utilizing 32 non-contrast CT series of which 31 were mapped onto one using mutual information (MI) as the similarity measure and thin plate splines (TPS) as warping transform. The image is segmented by adding the PA into a Bayesian framework based on a Markov random field (MRF) regularization term and solving maximum a posteriori estimation (MAP). Zhou et al. (2006), proposed a probabilistic model consisting of location and density probabilities. In this method, spatial relations between liver, bone structure and diaphragm are utilized for

defining a standard anatomical structure surrounding the liver with this anatomical structure being used as a reference with all 132 cases being deformed to it. Density probabilities of liver intensities are assumed as Gaussian and calculated utilizing the regions under PA. Afterwards, both probabilities are employed for segmenting the liver.

Slagmolen et al. (2007) proposed a PA and corresponding intensity atlas utilizing affine registration based on maximization of mutual information (MI) followed by a non-rigid registration utilizing B-splines via MI and surface distance between the reference segmentation and the floating image segmentation as a similarity metric. However, as in this PA is not directly build on the image to be segmented, an additional step is required to register both intensity atlas and PA onto the image of interest and then final segmentation is obtained by thresholding the PA.

Van Rikoort et al. (2007) proposed an automatic liver segmentation method combining non-rigid multi-atlas segmentation with voxel classification. Within an automatically selected region of interest, the voxels are labeled as liver or non-liver tissue by a k-Nearest Neighbors (kNN) classifier (Cover and Hart 1967), thresholding is utilized for detection of bones and the lungs as segmentation is limited to a fixed area under the lung. For PA building, twelve training series were registered to the test case using a B-spline model with a negative mutual information cost function utilizing parzen window estimation with a kNN classifier employed in the second stage. Afterwards, a feature vector including second order gradient and Gaussian derivatives and three spatial features that represent the percentage of the probabilistic segmentation of above, next or behind of the particular voxel is computed. The feature vector is then used in a kNN classifier and the segmentation is refined by post-processing with the morphological operations and smoothing functions.

Okada et al. (2008a) proposed a method combining PA and SSM. Registrations and construction of PA are done utilizing manually segmented abdominal cavities with point-based non-rigid registrations. PA has been utilized in voxel based segmentation as proposed by Zhou et al. (2006). To achieve a more flexible SSM, Okada et al. (2008a) proposed a multi-level SSM (ML-SSM) with landmark points being divided into N sub-shapes at every level and SSMs being computed for each of the sub-shapes. After the initialization by the PA based segmentation, their method searches for boundaries using intensity profiles and fits SSM to each patch. Okada et al. (2008b) later improved the performance of his segmentation by introducing a multi-organ SSMs (MO-SSMs) in a similar manner to multi-level-SSM. Spatial normalization for PA and construction of SSMs are achieved by defining a hierarchy of organ structures (i.e. abdominal cavity, liver and gallbladder/vena cava). For segmentation, initial parameters for ML-SSMs are found for each patch and for each organ and then refined by MO-SSMs with combining adhesiveness constraints of liver and other structures in the corresponding patches. The algorithm was able to provide better segmentation in the regions near vena cava and gallbladder as local variations these regions can be modeled more efficiently.

Linguraru et al. (2009) proposed a PA by normalizing organ coordinates relative to the positions of the xiphoid. Affine transform followed by non-linear registration based on B-splines deforms the atlas to the reference image, then final segmentation result is obtained by thresholding the atlas. Li et al. (2010) proposed a probabilistic liver atlas combined with a rib cage atlas with relatively rigid characteristics. In this implementation, problems of mapping derived from the variability in the liver shape are avoided by achieving a more accurate mapping of probabilistic atlas onto the input CT volume. For segmentation, probabilistic atlas mapped onto the image by utilizing rib-cage atlas with affine transformation and following the method proposed by Zhou et al. (2006). To achieve a refined segmentation, a level set based method is utilized in the post-processing step.

### 6.3 Geometric deformable model and level set based methods

Geometric deformable models also known as active contours proposed by Caselles et al. (1997) and level sets proposed by Osher and Fedkiw (2006) relying on boundary tracking by dynamic variations have gained high popularity in medical image segmentation. However, unlike active contours where a parametric characterization of contours are utilized, level set methods embed them as a time-dependent partial differential equation (PDE) function (Chan and Vese 2001; McInerney and Terzopoulos 1996; Wu et al. 2009). In level set formulation, the boundary of an object is embedded as zero-level set of a time-dependent function and this function is then evolved utilizing various speed functions. Speed function is the function specifying the speed at which the contour evolves along its normal direction. Furthermore, implicit versions of SSMs that are calculated in the space of signed distance functions can be utilized for embedding prior information into level set evolution (Leventon et al. 2000). Algorithms based on active contours can be considered as one of the most utilized and explored segmentation methods (Tsai et al. 2003; Al-Shaikhli et al. 2015; Li et al. 2011, 2014b).

Pan and Dawant (2001) proposed a liver-specific speed function for liver segmentation. The goal being the incorporation of memory into static edge function for slowed evolution of the contour as it passes the edges and to utilize a priori information based on other organs. It was shown that by utilizing this speed function, the contour was able to stop at weak boundaries and at spurious edges between ribs, liver and muscle. Saddi et al. (2007) proposed an implicit SSM and an appearance model consisting of inside and outside pixel distributions. The segmentation is parameterized with principal component analysis (PCA) coefficients, translation and rotation. The distribution of PCA coefficients (model feasibility) is modeled by kernel method corresponding to manifold learning. The energy to be minimized is defined as the sum of the cost of inside/outside pixel distributions and the probability of the corresponding PCA model feasibility. Wang et al. (2016) proposed an automatic liver segmentation algorithm utilizing level sets where initial liver segmentation is obtained using a probabilistic atlas approach with a maximum a posteriori classification. The segmentation is then refined using a shape and intensity prior based level set approach.

Garamendi et al. (2007) proposed a modified inside and outside regional models of Chan–Vese algorithm (Chan and Vese 2001) for utilization of local information around each voxel. Chi et al. (2007) proposed a 2.5D gradient vector flow (GVF) snake (Xu and Prince 1998), combining the GVF with the vector field from distance transform. Starting from the upper slice, distance transform vector field attracts snake to the vicinity of the boundary, then the segmentation is refined via GVF. Furukawa et al. (2007) proposed a method based on classifying tissues using a Gaussian mixture model (GMM) and a refined segmentation by active contours. An additional distance term from the skin is used for active contour evolution. Lee et al. (2007) proposed a method based on a region growing algorithm followed by active contours for a refined segmentation. The level set method proposed by Wimmer et al. (2007) needs several user defined contours and obtains a shape model by interpolating these contours via radial basis functions. This shape model consequently ensures that level set does not evolve too much from the initial contour. Wimmer et al. (2008) later proposed a liver segmentation algorithm utilizing an implicit version of appearance models in SSMs. For all grid points in narrowband around zero level set, boundary profiles are calculated and probabilities are assigned according to the learned appearance model. All boundary point candidates are projected back to the zero level set and the boundary point with the highest probability is kept along each path, the obtained probability map is used in GVF.

Massoptier and Casciaro (2008) proposed an active contour method based on basic image processing techniques such as thresholding and morphological operations. Wimmer et al. (2009) later proposed an active shape model based on nonparametric density estimates. As the boundary model, implicit version of kNN based intensity profile probabilities proposed by (Van Ginneken et al. 2002) are utilized. Region model is built utilizing a cascade of boosted classifiers and the result of classifiers are used as a dilatation or erosion of the surface of the level set equation. Furthermore, using Parzen density estimation for determining shape probability, shape information is added to level set evolution. Song et al. (2009) proposes a patient specific b-spline surface models from a pre-segmented image. Three B-spline based surface models are fitted to heart-liver boundary, liver right lobe boundary and lower liver surface on the pre-segmentation image. Utilizing graph-based optimal surface detection algorithm (Zhang et al. 2010), the surface models are further deformed to real pre-segmentation boundaries. The tissues outside the deformed model are removed from the pre-segmentation image and the remaining part used as initialization for level set evolution.

Suzuki et al. (2010) proposed a two-step automatic method where initial liver segmentation is achieved using fast marching level set and then refined using a geodesic active contour level set algorithm. Platero et al. (2011) proposed a variation of level set where shape priors are incorporated into edge-based and region-based models. The smoothness of the region of interest and the boundary length are considered in the energy function, describing a more specific boundary shape. Jimenez et al. (2011) proposed an optimized level set where the level set parameters are defined at each stage depending on the resolution step by means of a multi-curvature, multi-growth strategy and a refined segmentation by correcting the fine detail during the last multi-resolution level.

### 6.4 Region growing methods

Compared to more sophisticated methods, region growing methods are still able to provide competitive results (Rusko et al. 2007; Susomboon et al. 2007). Starting from a pre-identified small region called seed region and based on some pre-defined criteria, they operate by adding new voxels seeded region. However, region growing methods often fail in the presence of weak boundaries resulting in leakages. As a result, the segmentation needs to be refined by several pre/post processing steps.

Rusko et al. (2007) proposed an advanced region growing method for automatic liver segmentation where the intensity distribution of the liver is estimated by histogram analysis. Afterwards, the estimated intensity range is used to threshold the image and obtain an initial region of interest, a new voxel is added to the region if all voxels in a 5mm diameter are in the estimated intensity range. However, this method requires several post-processing steps especially near vena-cava and lungs to stop or correct the leaking. Rusko et al. (2009) later improved this method by utilizing multiphase CT images. Susomboon et al. (2007) proposed an automatic method utilizing clustering, voxel classification and region growing to segment liver. The expectation-maximization (EM) algorithm is used to define confidence intervals for different intensity distributions of tissues such as air, bone, fat and soft-tissue. The region with the highest probability of being the liver tissue is used as the seed region for a 2D region growing process where new voxels are added to the region if all voxels in its $9 \times 9$ voxel neighborhood are in the estimated confidence interval.

Beck and Aurich (2007) proposed a 3D region growing technique based on a nonlinear coupling criterion, which is the weighted intensity difference of a neighborhood to the seed intensity. Weights are assigned by a non-normalized Gaussian function of spatial distance and a non-normalized Gaussian function of intensity difference. The main disadvantage of

this method is the high level of user interaction to refine segmentation obtained by region growing due to excessive leakage. Chi et al. (2007) proposed a region growing technique with surface smoothness constraints and a rule-based system for identification of the region of interest for seeding. Unnecessary regions were extracted based on a predefined set of rules that can incorporate spatial features, estimations on intensity distribution and relations between neighboring organs. The extraction is done in the following order: background air, lungs and other intrabody air, subcutaneous fat and muscle layer, bones within muscle layer, aorta, spine, heart and liver. Based on the heart location, the right side of the liver sitting below the heart is used as an initial seeding region and leakage is prevented based on other segmented regions such as fat. However, there is room for improvement as there is a need to systematically optimize the rules of the proposed method.

Pohle and Toennies (2001) proposed an automatic segmentation based on region growing that learns its criteria for adding pixels from the characteristics of the region of interest. However, the proposed method cannot handle livers with inhomogeneity (such as pathological livers) leading to under segmentation. Mortelé et al. (2003) and Rusko et al. (2007) later expanded the method proposed by Pohle and Toennies (2001) utilizing a prior information. Based on anatomical information and gray level intensity range, heart and liver are separated followed by an improved region growing method for segmenting the liver. Although the post-processing steps proposed by the authors are able to correct the under segmentation on pathological livers with small tumors, the presence of large tumors will result in under segmentation. Kumar et al. (2013b) proposed a method based on region growing where the image is eroded and the center point of the largest connected region is used as the initial seeding region. The threshold range for the region growing algorithm is estimated by a Gaussian model and the results are post-processed to correct the segmentation.

### 6.5 Graph cut based methods

Graph Cut (GC) segmentation proposed by Boykov et al. (2001) is an alternative to boundary based segmentation methods, gaining popularity in medical image segmentation tasks. Being a semi-automatic segmentation the user is required to provide the seeds representing the background and the object to be segmented, GC represents the image pixels as nodes on a graph with weighted edges representing the adjacency between the pixels. By finding the minimum cost function between all possible cuts of the graph, the GC segments the image into background and the object. GC also offers the ability to interactively edit the segmentation result, making it a desirable method for clinical applications.

Beichel et al. (2007) proposed a graph cut segmentation process utilizing two refinement steps, requiring high user interaction as regional term and boundary term for graph-cut is obtained by user-selected seed points. Massoptier and Casciaro (2007) proposed a graph cut segmentation method initialized by adaptive thresholding. Initial liver location is detected by choosing the biggest connected component by thresholding the image using mean and standard deviation of liver while other regions are considered as background. Shimizu et al. (2010) proposed a combination of statistical atlas-based approach and graph cuts algorithm. Prior shape is estimated by utilizing the PA proposed in (Park et al. 2003) and then an implicit SSM is fitted as proposed in (Leventon et al. 2000).

### 6.6 Gray level based methods

Leveraging manually segmented liver slices, statistical analysis such as histograms can be utilized to get an estimation of gray scale intensity distribution of the liver. Based on this

intensity distribution, an initial liver outline is segmented followed by a refined segmentation by B-splines, active contours or other methods.

Lim et al. (2004, 2005, 2006) proposed several gray level methods for automatic liver segmentation based on intensity distribution estimated from a training dataset. Using prior information, initial liver location is estimated followed by k-means clustering algorithm and morphological operations to extract the liver boundaries attached to other body parts. The liver segmentation is then refined by an active contour based on liver intensity distribution and pattern features. Lee et al. (2003) proposed an automatic method where, based on spatial information and gray levels of pixels, an unsupervised contextual neural network is used for segmentation of different abdominal organs such as the liver. Based on spatial properties of each organ (size, shape, etc.) and using seven fuzzy rules, the boundaries of each organ is identified. Although, in practice this method was not able to achieve acceptable accuracy. Liu et al. (2005) proposed a method where the liver is extracted based on histogram analysis and intensity distribution of the liver acquired from a training dataset. The liver outline is then refined by morphological operations to remove other organs attached to liver boundaries. A gradient vector flow (GVF) based on initial boundary edges detected by a canny edge detector is then utilized for a refined but not a final segmentation. Although the method is automatic till this point, refined and final segmentation is done in a semi-automatic manner where the user selects CT slice with the best segmentation containing a large liver area and the remaining slices are refined iteratively based on the liver mask from the user selected slice.

Seo and Park (2005) proposed a left partial histogram threshold (LPHT) algorithm for automatic liver segmentation in contrast-enhanced CT imaging. Adaptive multi-modal thresholding is utilized for finding the gray level intensity range estimates for the liver followed by morphological operations for a refined boundary segmentation. Kim et al. (2007) proposed an automatic method where a region of interest in each CT slice is selected based on histogram analysis and intensity distribution of the liver acquired from a training dataset followed by a watershed algorithm for extraction of liver boundaries. Final segmentation is achieved by combining the segmented regions and using a priori information about the liver location and area. Campadelli et al. (2009) proposed an automatic segmentation method based on gray levels and a priori information about the location and area of abdominal organs combined with a rule-based system. Based on prior information, the heart is segmented then abdomen is divided into five labeled regions and an edge map is created for each region. Based on the assumption that abdomen organs have a Gaussian distribution of gray level intensities, a region growing algorithm is used to segment different organs. Foruzan et al. (2009) proposed a four step automatic method where the statistical parameters of the liver are calculated using the expectation maximization (EM) algorithm on a CT slice containing a large liver region. By extracting the heart and ribs, the region of interest of the liver is defined followed by a double thresholding approach where the liver intensity range is divided into two overlapping ranges. Liver candidate pixels are then identified using a decision table and refined by an anatomical based ruling system.

### 6.7 Methods incorporating machine learning algorithms

Apart from the mentioned methods, there are some other successful methods for segmenting liver tissue, often combining several methods together. Tsai and Tanahashi (1994) proposed a neural network (NN) based method where regional histograms are utilized as features. However, on its own, NN is not adequate to determine liver contour requiring exhaustive post-processing steps for a refined segmentation. Prior information about the location and

area of liver is utilized for the removal of unwanted and isolated parts, the liver boundary is then segmented. For achieving a smooth boundary, morphological operations followed by b-spline smoothing are utilized. Gao et al. (1996) proposed a rule based liver segmentation algorithm utilizing histogram analysis and thresholding. The intensity and shape based rules are incorporated into the thresholding algorithm to include or exclude different regions corresponding to different abdomen organs.

Schmidt et al. (2007) proposed an automatic approach using a scripting language that defines a set of intensity distributions, neighborhood relations and geometric features in order to successively segment different parts of CT data. Freiman et al. (2008) proposed an automatic method that iteratively applies a multi-class Bayesian classification. As a first step, Intensity models for liver, tumor and the other regions are created. Next, the posterior probabilities for each voxel are calculated by previously obtained multi-class distribution and using a uniform distribution for prior model. Finally, MAP rule is applied separately to two main classes and the results are combined followed by a final step that involves using adaptive morphological operations and active contours for fine-tuning. In a different work, Florin et al. (2007) proposed an automatic approach using a shape model that captures liver shape variations using a small number of carefully chosen slices. The idea is to reconstruct the whole 3D surface in reference space by selecting a minimal set of 2D contours along with an interpolation function. Schenk et al. (2000) proposed a semi-automatic segmentation method based on livewires (Falcão et al. 1998). A few slices (including top and bottom) are segmented via livewire in real time by an operator. Then the remaining slices are interpolated from segmented slices using distance transforms of those slices. Maklad et al. (2013) proposed an automatic approach method based on an initial identification of liver using the blood vessel information and histogram fitting using a variational Bayesian Gaussian mixture model. Chartrand et al. (2014) proposed a semi-automated method where an initial liver shape is generated by a few user specified contours followed by template matching. A geometric model is then fit iteratively based on a Laplacian mesh optimization framework, segmenting the final liver boundaries.

Goryawala et al. (2014) proposed an automatic 3D liver segmentation method where a k-means based clustering method is utilized in generating a region of interest followed by a region growing algorithm for initial segmentation followed by a localized contouring algorithm for a refined segmentation. Li et al. (2014b) proposed an automatic 3D liver segmentation method where an initial liver boundary is detected using a total variation with the L1 norm (TV-L1) followed by a level set method utilizing both local and global energy functions. For a refined segmentation, a texture analysis method based on gray level co-occurrence matrix (GLCM) is utilized. Li et al. (2014c) proposed an automatic liver segmentation method where the initial liver location is identified using a voxel-based AdaBoost classifier followed by SSM registration for initial segmentation. Free-form deformations based on deformable simplex mesh segmentation is then utilized for refining the segmentation. Mostafa et al. (2015) proposed an automatic liver segmentation method where initial liver boundaries are segmented based on an artificial bee colony clustering followed by morphological operations. For a refined segmentation, region growing is utilized in the last step. Shi et al. (2015) proposed an automatic liver segmentation method based on multilevel local region-based sparse shape composition with initialization based on the shape of blood vessels. The idea is that the liver vessels can be used to acquire patient specific prior information such as shape and size of the liver, providing a more accurate initialization. Al-Shaikhli et al. (2015) proposed an automatic liver segmentation method based on an updated level set cost function embedding global and local image information. The initial liver region of interest is identified using a prior information based on a gray level co-occurrence matrix (GLCM) followed by

level set segmentation for obtaining the final liver boundary. Xu et al. (2015) proposed an automatic segmentation method for abdominal organs including liver based on Multi-atlas segmentation (MAS) based performance level estimation (SIMPLE) method.

Li et al. (2014a) proposed an automatic segmentation method on graph-based Dirichlet integral. Wang et al. (2015a) proposed an automatic liver segmentation method where an initial liver boundary is identified using gray level methods. Based on deformable simplex model (DSM), adaptive mesh expansion model (AMEM) is utilized for final segmentation of liver boundaries. Huang et al. (2014a) proposed an automatic liver segmentation method where an initial liver boundary is identified using a trained voxel-based AdaBoost classifier followed by Free-form deformation for a refined segmentation. Anter et al. (2014) proposed an automatic liver segmentation method where an initial liver boundary is detected using fuzzy c-means clustering followed by morphological operations for a refined segmentation.

### 6.8 Summary

While many authors stress the value of prior information in liver segmentation, region growing strategies nevertheless offer good results because of their ability to adapt to the specific characteristics of each image. However, region growing strategies have the disadvantage of badly handling pathological livers with lesions. PA and SSM both utilize prior information on the liver while it seems that SSM achieves better results. PAs indeed offer less substantial results, but their accuracy could be improved by utilizing better standardization techniques.

Moreover, PAs not only model the liver but are also often utilized in the modeling of other abdominal organs. Whereas PAs mainly handle non-contrast images, SSMs shows better results while working on enhanced CT images. Finally, despite the advantages mentioned, SSMs based approaches face two major difficulties, the initialization of an SSM is complex while very crucial and the possible deformations of the liver modeled by an SSM are limited. The deformation limitations prevent SSM capturing of the high variability of the liver shapes. To overcome this problem SSMs approaches often rely on an additional step for obtaining a finer segmentation contour.

Automatic methods based on SSMs, PAs and other deformable models require a large training dataset for modeling the different variation of livers, especially pathological livers where the liver shape and anatomical structures inside the liver (different tumors) can differ from regular livers by a large degree. Furthermore, semi-automatic methods were generally regarded as more robust especially in the case of irregular livers as these segmentation methods rely on some level of user interaction. However, as these semi-automatic methods are reliant on the operator skill, their final segmentation can differ from one operator to another. The main advantage of an automatic segmentation over semi-automatic and manual segmentations is the reproducibility as there is no human interaction and the segmentation can run in the background without the need for an operator, making them more desired for clinical applications. On the other hand, since the Sliver'07 challenge, many automatic segmentation methods have been proposed that are able to achieve similar and in some cases better results compared to many semi-automatic methods proposed previously, even surpassing the accuracy of manual segmentation reported in Sliver'07 (Heimann et al. 2009). These new methods often include or can be adapted to provide the ability to alter the segmentation in a semi-automatic mode if the final result is not satisfactory while in many of these newer methods the pathological livers are the main focus. Based on a comparison between recently published automatic liver segmentation methods, it seems that most of these methods are able to achieve a DSC of 0.94 representing a very good segmentation accuracy compared to radiologist segmentation. Furthermore, it can be observed that standardized dataset is still

the main concern as many authors used their own dataset even during the Sliver'07, making a direct comparison between these methods difficult. Table 1 represents some of the most accurate liver segmentation methods.

## 7 Liver tumor segmentation

Liver tumor segmentation is considered a more challenging task as a wide range of tumor tissue appearances makes for a difficult segmentation. Moreover, this segmentation is usually done on a noisy background as the low contrast of liver tumors mandates the use of contrast enhanced CT scans, increasing the amount of noise in images. Figure 2 illustrates the level of background noise in a typical contrast enhanced CT image.

This contrast enhancement is achieved by injecting the patient with a harmless contrast agent, with the goal of enhancing the contrast between the liver and tumor tissues. However, this method of enhancement has its own drawbacks. First, the characteristics and enhancement of tumoral tissue in each phase depends on the type of the lesion. Then, an experienced radiologist should carefully control and monitor the time between injection and image acquisition, so that the lesion is better seen during the desired phase of the CT scan. From the diagnostics point of view, using contrast enhanced CT imaging imposes an additional problem: the uneven enhancement due to anatomical differences between different tumors. Furthermore, some lesions do not have clearly visible edges (e.g. diffuse cancers or some HCCs), limiting the effective use of edges based segmentation methods as sole segmentation approach. Moreover, the native noise in CT images and uneven enhancements in contracted enhanced CT images severely limits the tissue type determination using the voxel intensity.

Unfortunately, compared to many liver segmentation methods proposed, liver tumor segmentation has received low interest from researchers. This can be attributed to the difficulties associated with liver tumor segmentation and an interesting lack of public datasets, limiting the development of tumor segmentation methods. While more recent methods usually rely on a pipeline of different techniques to achieve an accurate liver tumor segmentation, most of the previously proposed methods can be seen as relying on only basic segmentation concepts. In order to promote the problem of liver tumor segmentation, a challenge known as the Liver tumor segmentation challenge 2008 (LTSC'08, 2016) was introduced as a part MICCAI 2008 workshop on medical imaging following their liver segmentation challenge from previous year. Many of the more evolved liver tumor segmentation methods were proposed as a result of this workshop. Thus, this challenge will be briefly introduced. Various methods proposed for liver tumor segmentation is discussed in the following sections.

### 7.1 Thresholding based methods

Soler et al. (2001) proposed the first threshold technique for segmentation of the liver tumors as part of a liver surgery planning system. Seo and Park (2005) proposed a simple thresholding method, then an optimal threshold for tumor segmentation was proposed by Park et al. (2005). Ciecholewski and Ogiela (2007) later proposed the use of histogram equalization for simplifying the choice of a threshold value. Nugroho et al. (2008) proposed a threshold maximizing the variance between classes. Choudhary et al. (2008) relies on cross-entropy for thresholding, level set method is used for a refined segmentation. Moltz et al. (2008, 2009) proposed a method for delineating the tumor boundaries using adaptive gray level thresholding combined with model-based morphological processing. Huang et al. (2011), Kumar et al. (2013b) and Rusko et al. (2007) have also proposed tumor segmentation methods

**Table 1** Comparison between some of the more accurate methods published on liver segmentation

| Author | Method | Used specific type of data | Mean VOE | Mean RVD | Mean DSC | Mean runtime (min) |
|---|---|---|---|---|---|---|
| Wimmer et al. (2007), semi-automatic | Level set | No | $4.25 \pm 0.6$ | $0.59 \pm 1.65$ | Not mentioned | Not mentioned |
| Maklad et al. (2013), semi-automatic | Blood vessel information and histogram | No | $4.33 \pm 0.7$ | $0.28 \pm 0.87$ | Not mentioned | Not mentioned |
| Beichel et al. (2007), semi-automatic | Graph cuts | No | $5.2 \pm 0.9$ | $1 \pm 1.7$ | Not mentioned | 36 |
| Chartrand et al. (2014), semi-automatic | Geometric model | No | $6.7 \pm 1.2$ | $1.7 \pm 1.6$ | Not mentioned | 3 |
| Goryawala et al. (2014), semi-automatic | Region growing | Pathological | Not mentioned | $-2.78 \pm 4.39$ | $0.92 \pm 0.01$ | Not mentioned |
| Erdt et al. (2010), semi-automatic | SSM | No (3Dircadb) | $10.34 \pm 3.11$ | $1.55 \pm 0.49$ | Not mentioned | 0.8 |
| Li et al. (2014b), automatic | Level set | Healthy | $2.7 \pm 2$ | $2.8 \pm 4$ | Not mentioned | Not mentioned |
| Li et al. (2014a), automatic | SSM | No | Not mentioned | Not mentioned | $0.922 \pm 0.011$ | Not mentioned |
| Mostafa et al. (2015), automatic | Artificial bee colony clustering | Healthy | $6.3 \pm 2$ | Not mentioned | Not mentioned | Not mentioned |
| Shi et al. (2015), automatic | Geometric deformable model | No | $7.05 \pm 2.2$ | $1.73 \pm 4.33$ | Not mentioned | 8.5 |
| Kainmüller et al. (2007), automatic | SSM | No | $6.1 \pm 2.1$ | $-2.9 \pm 2.9$ | Not mentioned | 15 |

**Table 1** continued

| Author | Method | Used specific type of data | Mean VOE | Mean RVD | Mean DSC | Mean runtime (min) |
|---|---|---|---|---|---|---|
| Al-Shaikhli et al. (2015), automatic | Level set | No | $6.44 \pm 0.6$ | $1.53 \pm 1.7$ | Not mentioned | Not mentioned |
| Wang et al. (2015a), automatic | Geometric deformable model | No | $6.8 \pm 2.7$ | $2.7 \pm 0.9$ | Not mentioned | Not mentioned |
| Huang et al. (2014a), automatic | Geometric deformable model | No | Not Mentioned | Not mentioned | 0.925 | Not mentioned |
| Xu et al. (2015), automatic | Geometric deformable model | No | Not Mentioned | Not mentioned | 0.93 | 90 |
| Li et al. (2014a), automatic | Graph based | No | Not Mentioned | Not mentioned | $0.937 \pm 0.01$ | Not mentioned |
| Anter et al. (2014), automatic | FCM | No | Not Mentioned | Not mentioned | 0.94 | Not mentioned |
| Wang et al. (2015b), automatic | Geometric deformable model | No | Not Mentioned | Not mentioned | $0.94 \pm 0.03$ | 1.5 |
| Chung and Delingette (2013), automatic | Geometric deformable model | No | $12.99 \pm 5.04$ | $-5.66 \pm 5.59$ | Not mentioned | Not mentioned |
| Song et al. (2014), automatic | Geometric model | Not Mentioned | $4.1 \pm 0.67$ | Not mentioned | Not mentioned | Not mentioned |
| Shi et al. (2015), automatic | Geometric deformable model | No (3Dircadb) | $8.74 \pm 0.37$ | $2.41 \pm 1.71$ | Not mentioned | 8.5 |
| Moghbel et al. (2016a), automatic | Graph cuts | No | $4.47 \pm 1.7$ | $2.38 \pm 2.61$ | $0.94 \pm 0.01$ | 3.5 |

**Table 1** continued

| Author | Method | Used specific type of data | Mean VOE | Mean RVD | Mean DSC | Mean runtime (min) |
|---|---|---|---|---|---|---|
| Moghbel et al. (2016a), automatic | Graph cuts | Pathological | $5.95 \pm 2.56$ | $7.49 \pm 9.63$ | $0.91 \pm 0.02$ | 4 |
| Wang et al. (2016), automatic | Level sets | No | $7.57 \pm 0.96$ | $-1.83 \pm 2.02$ | Not mentioned | 7 |
| Saxena et al. (2016), automatic | Atlas based | Pathological | 13 | Not mentioned | Not mentioned | Not mentioned |
| Wu et al. (2016), automatic | Graph cuts | No | 7.87 | 1.31 | Not mentioned | 0.5 |
| Liao et al. (2016), automatic | Graph cuts | No | $5.5 \pm 0.7$ | $-1.7 \pm 1.9$ | Not mentioned | Not mentioned |
| Lu et al. (2016), automatic | Graph cuts | No | 5.9 | 2.7 | Not mentioned | Not mentioned |
| Lu et al. (2016), automatic | Graph cuts | No (3Dircadb) | 9.36 | 0.97 | Not mentioned | Not mentioned |
| Manual segmentation (Heimann et al. 2009) | Manual | No | 6.4% | 4.7% | Not mentioned | Not mentioned |

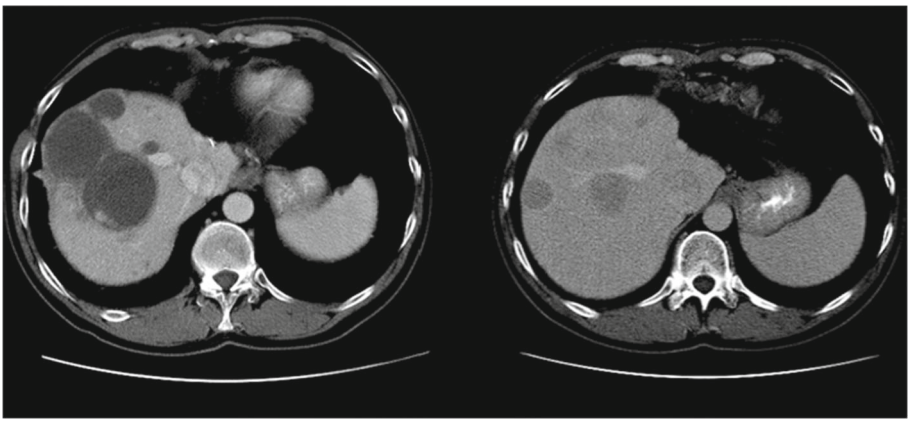

**Fig. 2** As it can be seen, contrast enhanced liver CT image can have high background noise

where the initial tumor boundaries are segmented using histogram analysis and thresholding followed by post processing steps for a refined segmentation. The method proposed by Abdelmassieh et al. (2010) utilizes Isodata threshold technique for segmentation of tumors from CT images. The image is filtered using Gaussian smoothing followed by a multilevel Isodata threshold for converting the image into binary for detection of tumors.

### 7.2 Region growing and deformable model based methods

Region growing and active contour techniques are also amongst the popular methods for liver tumor segmentation as they provide segmentations with higher accuracies and are easy to implement. Various methods have been proposed using variations of region growing algorithms in either 2D or 3D and with different energy functions. Wong et al. (2008) proposed a 2D region growing technique with knowledge-based constraints for tumor segmentation. Qi et al. (2008) proposed a method based on region growing algorithm utilizing bayesian decision rule with PDF models for the tumors that are updated during the algorithm. Ben-Dan and Shenhav (2008) proposed an active contour based tumor segmentation using a weighted function of the probability of each pixel being inside the tumor region. Fernández-de-Manuel et al. (2009) also proposed a similar, active contour based tumor segmentation method. However, these methods differ by the strategies and space where the active surfaces are defined. Ben-Dan proposed a probability space where probabilities are defined by a joint likelihood ratio modeling the tumor intensities. On the opposite, Fernandez uses a level set technique for tumor segmentation. Linguraru et al. (2012b) proposed a tumor segmentation method where initial tumor boundaries are detected by histogram analysis and active contours are used for a refined segmentation.

Level set methods are also amongst popular segmentation techniques with a number of proposed methods. Smeets et al. (2008) proposed a level set algorithm based on statistical pixel classification with supervised learning for the segmentation of tumors. Jimenez et al. (2011) proposed a multi-resolution 3D level set technique coupled with adaptive curvature technique for the classification of the pixels into tumor and background. Choudhary et al. (2008) proposed a method using cross-entropy for thresholding followed by level set method for a refined segmentation.

### 7.3 Machine learning based methods

Due to the variability of the tumors and difficulties in defining thresholds, machine learning techniques have also been proposed for tumor segmentation. These machine learning techniques have been used in two ways, either clustering of similar voxels inside an image or to defining prior models for the segmentation. Massoptier and Casciaro (2008) proposed a method using k-means clustering technique to segment the tumor inside the liver. Taieb et al. (2008) proposed bayesian classification of tumors for getting an initial segmentation followed by active contours for refinement. Häme (2008) uses fuzzy c-means clustering (FCM) with spatial smoothing followed by deformable models for a refined segmentation. Häme later improved his method employing shape prior with non-parametric intensity distribution estimation and a hidden markov measure field model (Häme and Pollari 2012). Zhou et al. (2008) proposed a method propagating an initial segmentation on one slice using SVM while requiring an update after segmentation of each slice. Shimizu et al. (2008a, b) and Li et al. (2006b) proposed labelling of voxels as tumor and background using an AdaBoost classifier. The method proposed by Shimizu et al. uses a set of image features such as texture while the method proposed by Li et al. is based on image intensity profiles.

Smeets et al. (2008) proposed using level sets with a speed dependent on fuzzy classification for tumor segmentation. Jolly and Grady (2008) proposed a three steps segmentation method beginning with user input for estimation of gray level distributions followed by a 2D fuzzy connectedness segmentation. As the final step, a refined 3D segmentation is obtained using random walkers method. Choudhary et al. (2008) proposed a semi-automatic technique where an initial Watershed algorithm is followed by minimum entropy-based region growing technique for an initial segmentation and level set method for a smooth outline. Yi et al. (2010) proposed the use of a local entropy-based method coupled with morphological operations for segmentation of liver tumors. Taieb et al. (2008) proposed a method using a multi-resolution, multiclass bayesian classification technique followed by morphological operations for a refined segmentation. Although the method is considered semi-automatic, the amount of required user input is minimal.

Qi et al. (2008) proposed another semi-automatic bayesian based approach for segmentation of liver tumors. In this method, initial tumor region is segmented by modeling the probability density function of the tumor as a series of Gaussian distributions followed by a 3D seeded region growing algorithm. The seeds for the region growing algorithm are selected manually and updated during the region growing process. Vorontsov et al. (2014) proposed an automatic segmentation method where initial tumor segmentation is done using an SVM classifier followed by markov random field based omnidirectional deformable surface model for a refined segmentation. Masuda et al. (2011) proposed an automatic segmentation method where initial tumor segmentation is done using expectation-maximization/maximization of the posterior marginal (EM/MPM) algorithm followed by shape filters for a refined segmentation. Huang et al. (2013) proposed a semi-automatic segmentation method where tumor segmentation is done using Extreme Learning Machine (ELM) algorithm. Stawiaski et al. (2008) proposed an interactive tumor segmentation method using graph cuts for an initial segmentation and watersheds for a refined segmentation. Huang et al. (2014b) later proposed a semi-automatic tumor segmentation method using an updated version of extreme learning machine (ELM) algorithm called random feature subspace ensemble ELM (RFSE-ELM) classifier. Other methods include interactive tumor segmentation utilizing intensity distribution combined with hidden markov fields (Häme and Pollari 2012), semi-automatic tumor segmentation with support vector machines with affinity constraint propagation (Freiman et al. 2011) and machine learning algorithms (Xu and Suzuki 2011). Automatic segmenta-

tion methods including a method utilizing watersheds and region growing (Anter et al. 2013) and another method with free-form deformations (Huang et al. 2014b). Various other techniques based on AdaBoost (Jingran et al. 2009; Li et al. 2006b) and Support Vector Machines (Zhang et al. 2011; Ben et al. 2010) have also been proposed for segmentation of the tumors.

### 7.4 Summary

Unfortunately, most of the current and previous research on tumor segmentation in CT imaging is focused on lung and lung node segmentation. This can be attributed to the difficulties associated with liver tumor segmentation and an interesting lack of public datasets. On the other hand, as manual segmentation of tumors by a radiologist is both time-consuming and tedious, many researchers utilize datasets with typically under 20 segmented tumors. To address these problems, a challenge was presented to different researchers by the medical image computing and computer assisted intervention society to segment liver tumors on clinical basis following their liver segmentation challenge from the previous year. Liver tumor segmentation challenge 2008 was a challenge aimed at the development of several liver tumor segmentation algorithms. Although as a result of this workshop many accurate automatic segmentation approaches were developed, surpassing the accuracy achieved by many semi-automatic methods, the accuracy achieved can be considered lower than expected compared to the accuracy of liver segmentation methods.

LTSC'08 included a CT dataset with 20 tumors in total. Unfortunately, the dataset has become unavailable due to lack of maintenance on the competition website while their liver segmentation dataset from the previous year is still accessible to researchers. This lack of dataset is apparent as most publications on the subject are from 2008 to 2010 with some publications afterwards. Recently, 3Dircadb dataset containing 120 tumors and MIDAS dataset containing 10 tumors, all segmented by expert radiologist has been made publicly available for researchers (compared to a total of 20 tumors from LTSC'08). Hopefully, with these new datasets more researchers will focus on developing more accurate liver tumor segmentation methods. Despite lots of attention, fully automatic liver tumor segmentation from a CT volume remains a challenging task, mainly because of the variability of the tumor shapes and the intensity patterns inside and in the neighborhood of the tumor. Ideally, tumor segmentation methods should also include a liver segmentation step as working inside a segmented liver envelope yields better results as previous works have shown that segmentation of liver tumors was more accurate when done inside liver only, in particular for automatic methods (Taieb et al. 2008; Schmidt et al. 2008; Qi et al. 2008; Ben-Dan and Shenhav 2008; Shimizu et al. 2008a, b; Smeets et al. 2008; Kubota 2008; Wong et al. 2008; Moltz et al. 2008; Stawiaski et al. 2008; Zhou et al. 2008). Table 2 represents some of the most accurate liver tumor segmentation methods.

Comparison of liver lesion segmentation methods is indeed very challenging as there is a large variety of possible error metrics for illustrating the performance of these segmentation methods. Some authors have considered the tumor detection rate as a representation of their methods performance instead of other measures such as VOE and RVD. Table 3 shows a comparison between these methods with the precision calculated by:

$$\text{Precision} = (\text{sum true positive})/(\text{sum true positive} + \text{sum false positive}) \tag{6}$$

Overall, any method with a precision of 50% or more can be considered as an efficient tumor segmentation method. However, it should be noted that most of the methods in Table 3 have not used the same dataset, making a direct comparison difficult. Moreover, some of these

**Table 2** Comparison between some of the more accurate methods published on liver tumor segmentation

| Author | Method | Number of tumors | Mean VOE | Mean RVD | Mean DSC | Mean runtime (min) |
|---|---|---|---|---|---|---|
| Linguraru et al. (2012a), automatic | Gray levels and geodesic active contour | 79 | Not mentioned | $12.4 \pm 12$ | $0.74 \pm 0.16$ | Couple of minutes |
| Vorontsov et al. (2014), semi-automatic | SVM and deformable surface model | 27 | Not mentioned | Not mentioned | $0.81 \pm 0.06$ | Not mentioned |
| Masuda et al. (2011), automatic | EM/MPM and shape filters | 15 | 37.165 | 30.65 | Not mentioned | Not mentioned |
| Shimizu et al. (2008a), automatic | AdaBoost classifier | 10 | 28.98 | 18.29 | Not mentioned | Not mentioned |
| Huang et al. (2013), semi-automatic | Extreme learning machine | 20 | 32.85 | 21.97 | Not mentioned | Not mentioned |
| Stawiaski et al. (2008), interactive | Graph cuts and watershed | 10 | 29.49 | 23.87 | Not mentioned | 8 |
| Zhang et al. (2011), semi-automatic | SVM | 10 | $26.31 \pm 5.79$ | $-10.64 \pm 7.55$ | Not mentioned | 0.5 |
| Häme and Pollari (2012), interactive | Intensity distribution combined with hidden Markov fields | 20 | $30.35 \pm 11.03$ | $2.43 \pm 1.41$ | Not mentioned | 15 |
| Zhou et al. (2010), semi-automatic | Region growing | 37 | $25.7 \pm 17.14$ | $17.93 \pm 27.78$ | Not mentioned | Couple of minutes |
| Huang et al. (2014b), semi-automatic | RFSE-ELM | 20 | $25.25 \pm 26.96$ | $11.89 \pm 17.41$ | Not mentioned | No info |

**Table 2** continued

| Author | Method | Number of tumors | Mean VOE | Mean RVD | Mean DSC | Mean runtime (min) |
|---|---|---|---|---|---|---|
| Moghbel et al. (2016b), automatic | FCM and graph cuts | 117 | $22.78 \pm 12.15$ | $8.59 \pm 18.78$ | $0.75 \pm 0.15$ | 16 |
| Moghbel et al. (2016b), automatic | FCM and graph cuts | 10 | $15.61 \pm 5.32$ | $4.02 \pm 11.10$ | $0.81 \pm 0.06$ | 16 |
| Average manual 5 radiologist segmentation, MIDAS | Manual | 10 | $9.80 \pm 8.02$ | $-2.54 \pm 0.46$ | $0.83 \pm 0.03$ | Not mentioned |
| Average manual human segmentation, LTSC'08 | Manual | 20 | 12.94 | 9.64 | Not mentioned | Not mentioned |
| Average manual 10 radiologist and technician segmentation, (Moltz et al. 2011) | Manual | Not mentioned | Not mentioned | 17 | Not mentioned | Not mentioned |

**Table 3** Comparison between the detection rate of the proposed method and some of the most accurate methods proposed for liver tumor segmentation

| Author | Detection rate (%) | False positive | Precision (%) | Used specific tumor type |
|---|---|---|---|---|
| Bilello et al. (2004), automatic | 80 | 0.8/CT slice | Not mentioned | Hypo-dense |
| Tajima et al. (2007), automatic | 98 | 2.1/case | Not mentioned | HCC |
| Massoptier and Casciaro (2008), automatic | 83 | 0.1/case | 93 | Hypo-dense |
| Militzer et al. (2010), automatic | 71 | 14/case | 17 | No |
| Masuda et al. (2010), automatic | 73 | 1.7/case | 30 | No |
| Casciaro et al. (2012), automatic | 92 | Not mentioned | Not mentioned | Hypo-dense |
| Linguraru et al. (2012a), automatic | 100 | 2.3/case | 71 | Metastases |
| Wu et al. (2012), automatic | 90 | 2.6/case | Not mentioned | No |
| Chi et al. (2013), automatic | 90 | 1.0/case | Not mentioned | No |
| Safdari et al. (2013), automatic | 84 | Not mentioned | 73 | No |
| Schwier et al. (2011), automatic | 78 | Not mentioned | 53 | Hypo-dense |
| Rusko and Perényi (2014), automatic | 91.5 | 1.7/case | 51.4 | No |
| Pamulapati et al. (2011), automatic | 100 | 3.1/case | Not mentioned | No |

methods have been developed using a specific tumor type and should not be considered as a complete liver tumor segmentation method.

## 8 Liver blood vessel segmentation

Analysis of 3D vasculature structure from volumetric images has received interest due to possible contributions towards a variety of medical applications. Accurate annotation of the blood vasculature structure can result in improved diagnosis and more accurate liver surgical and resection planning (Sonka and Fitzpatrick 2000; Kirbas and Quek 2003). In treatment options such as SIRT, knowing the 3D structure and branching of the blood vessels (especially those feeding the lesions) along with ability to display the liver and the tumor(s) in a 3D space can ease treatment planning as a more accurate map for the insertion point of the radioisotope can be generated (Gulec and Fong 2007). Many methods have been proposed for this segmentation including methods based on machine learning techniques, model based approaches and other algorithms.

Initially, skeleton-based methods have been used for locating and extracting the centerline of the blood vessel tree structure in CT images. These methods use one or more types of skeletonization techniques for obtaining a skeleton followed by thresholding for determining the blood vessel structure (Kawata et al. 1996; Tozaki et al. 1995). Vasculature extraction approaches using region growing methods that are based on intensity similarity and the spatial proximity between voxels are also popular (Selle et al. 2002). However, as these methods rely on voxel seeding, automatic segmentation initialization can be difficult. Methods based on deformable models such as level sets are amongst the most popular vessel segmentation methods (Luo et al. 2000; Malladi et al. 1996; Malladi and Sethian 1996; Toledo et al. 2000). Historically, although these methods are very popular for segmenting cardiac angiography, their use in liver vasculature extraction from CT images have been limited due to complex initialization (Selle et al. 2002). However, with recent advances in machine learning methods, deformable models are becoming very popular for liver vessel segmentation. Usually, an initial segmentation is achieved using machine learning algorithms such as pixel clustering methods and then refined by deformable models such as level sets (Selle et al. 2002).

Perhaps the most difficult aspect of vasculature structure segmentation methods can be considered as the validation. Validating vessel segmentation results are very difficult since these validations are generally obtained using corrosion casts that require expensive equipment and are very tedious to prepare and evaluate (Selle et al. 2002). An alternative validation technique could be manual segmentation of these blood vessels by an experienced radiologist. However, this would be a very tedious and time-consuming process considering the number of slices in a typical CT image of the liver. There are near thirty publications dealing with the hepatic vessel segmentation problem on CT. Amongst these, only some publications have validated their proposed method using only some (and not all) of the standard validation measures common in CT imaging with the majority of the remaining publications validating their method using a visual inspection of the accuracy of the segmentation (Beichel et al. 2004; Chi et al. 2011; Marcan et al. 2014). As no public dataset had existed for liver vessel segmentation prior to 3Dircadb, a quantitative comparison between different methods proposed for segmentation of hepatic vessels from CT images is difficult as a comparison would be more valuable if done using the same standard dataset with same validation criterion. Although some attempts have been made for standardizing liver and liver segmentation datasets and evaluation criterion by MICCAI in 2007 (Sliver'07) and 2008 (LTSC'08), no attempt has been made to introduce standardized hepatic vessel segmentation dataset while these vessels can play an important role in liver treatment planning as mentioned. Moreover, although the 3Dircadb dataset can be considered as the new benchmark for developing and evaluating different organ segmentation methods in CT imaging, it seems that it has not been used for developing and evaluating any hepatic vessel segmentation methods. Table 4 shows a comparison between different liver blood vessel segmentation methods. It should be noted that although the method proposed by Marcan et al. (2014) is validated using Magnetic resonance imaging (MRI), it can be easily adapted for use with CT imaging.

## 9 Computer assisted diagnosis (CAD) systems

Early attempts at using computer-based medical images analysis date back to 1960s, during that time many believed that a computer can potentially replace a physician and so, much effort was put in the development of computer-based diagnosis systems. However, computer-based artificial intelligence systems were at early stages of development and computers lacked

**Table 4** A comparison between different liver vessel segmentation methods

| Author | Dataset type | Mean VOE | Mean RVD | Mean ASD | Mean RMSD | Mean runtime (min) |
|---|---|---|---|---|---|---|
| Beichel et al. (2004), automatic | 1 Phantom | Not mentioned | $6.02 \pm 3.4$ | Not mentioned | Not mentioned | Not mentioned |
| Beichel et al. (2004), automatic | 1 Phantom | Not mentioned | $1.96 \pm 1.25$ | Not mentioned | Not mentioned | Not mentioned |
| Chi et al. (2011), automatic | 10 Clinical | $45.1 \pm 7.12$ | No info | $2.28 \pm 1.39$ | Not mentioned | 3 |
| Marcan et al. (2014), automatic | 6 Clinical using MRI | Not mentioned | Not mentioned | Not mentioned | $0.83 \pm 0.13$ | Not mentioned |

the computation resources, also advanced image processing techniques that exist today were not available during that period. As a result, the idea of using computers in medical diagnosis tasks was abandoned by many researchers. However as a result of increased computational capacity and the introduction of more advanced image processing techniques during the 1980s, the concept known as Computer assisted detection/diagnosis became widely popular amongst researchers. CAD is not aimed at replacement of the physician but rather works on the principle of aiding the physician by providing additional information about the abnormalities in patient data or by providing a diagnosis which can serve as a second opinion. CAD is currently employed in many aspects of daily clinical practice such as breast cancer, skeletal, brain and vascular disorders.

Gunasundari and Ananthi (2012) proposed a liver CAD for automatic classification of tumors into hepatocellular carcinoma (HCC) and hemangioma from CT modality using a probabilistic neural network (PNN) classifier utilizing a dataset containing 40 HCC and 30 Hemangioma CT slices. The liver is segmented using histogram analysis followed by morphological operations while FCM is used in tumor segmentation step. Feature extraction is done using a combination of gray level co-occurrence matrix (GLCM), biorthogonal wavelet and fast discrete curvelet transform (FDCT) techniques with tumor classification accuracy reported as 96% while this accuracy decrease to 88% if (FDCT) based features are excluded from the classifier. Although the addition of FDCT features can increase classification accuracy, computation and selection of FDCT features can be considered difficult and complex. Hameed and Kumar (2012) proposed a liver CAD for automatic classification of tumors into benign and malignant from CT modality using a probabilistic neural network (PNN) and pulse coupled neural network (PCNN) classifiers with feature extraction being done using GLCM. Tumor classification accuracy reported by PNN classifier is 84% while using same features, PCNN classifier was able to achieve an accuracy of 87%. While being faster than traditional neural networks, PNN suffers from dimensionality and require extensive feature selection to remove all irrelevant features from the input.

Kayaaltı et al. (2012) proposed a liver CAD for automatic classification of seven different stages of liver fibrosis from CT modality using support vector machines (SVM) and k-nearest neighbor (KNN) classifiers utilizing a dataset containing 116 CT series. Feature extraction is done using gray level co-occurrence matrix, discrete wavelet transform (DWT), and discrete Fourier transform (DFT). After feature extraction step, the median for each feature is calculated and data normalization is done followed by feature selection step using sequential forward floating selection (SFFS) process. Tumor classification accuracy reported by SVM classifier is 90% pairwise classification and 37% in stage detection while using same features, k-NN classifier accuracy of was not given. Thakre and Dhenge (2013) proposed a liver CAD for automatic identification of healthy and pathological livers from CT imaging. Livers are extracted using deformable contours followed by feature extraction step using GLCM. Modified probabilistic neural network (MPNN) is used as a classifier for distinguishing normal and abnormal livers. Unfortunately, the accuracy of the method was not given. Sharma et al. (2013) proposed a liver CAD for automatic classification of liver tissue into hepatic cyst, Hemangioma, hepatocellular carcinoma and healthy from CT images using confusion matrix and neural network (NN). Feature extraction is done using first order statistics (FOS), texture energy measures (TEM), gray-level dependence matrix (GLDM), fractal dimension measurements (FDM) and GLDM. However, they have not reported the accuracy of the proposed method.

Chen et al. (2013) proposed a liver CAD system for classification of normal and cirrhotic livers using shape analysis based on the idea of liver and spleen going under shape changes during the clinical course of liver cirrhosis. Feature selection is based on liver and spleen

shapes obtained by SSMs and support vector regression (SVR) on a CT dataset containing 25 normal and 19 cirrhotic cases. Using a nearest neighbor classifier, an accuracy of 89.5% was reported in the identification of liver cirrhosis. However, this accuracy can be increased by utilizing a larger dataset as SSMs based methods require large training samples. Duda et al. (2013) proposed a liver CAD for automatic classification of liver tissue into Cholangiocarcinoma, cirrhotic, hepatocellular carcinoma and healthy from multi-phased CT images corresponding to three acquisition moments (without contrast, arterial and portal phase of contrast agent propagation). Texture features are extracted independently for each phase using a total of nine different feature extraction methods. Using a classifier based on AdaBoost with a C4.5 tree, an accuracy of 90% was reported for the method.

Vincey (2013) proposed a liver CAD for automatic identification of healthy and pathological livers from CT imaging. Livers are extracted using region growing followed by feature extraction step. Hidden markov model (HMM) is used as a classifier for distinguishing normal and abnormal livers with an accuracy of 96.5%. Dankerl et al. (2013) proposed a comprehensive liver CAD system to retrieve tumors based on histology (benign, malignant), density (hypodense, hyperdense) and type (cyst, hemangioma, metastasis) from using a CT dataset containing 685 CT scans from 372 patients with 2325 liver tumors in total. They aim to provide a second opinion to the radiologist by retrieving similar tumors to the tumor being assessed and by providing the radiologist reports on the retrieved tumors. Their proposed method based on intrinsic random forest similarity classifier was able to achieve retrieval accuracies of 97.1, 91.4 and 95.5% for tumor density, histology and type, respectively.

Kumar et al. (2013a) proposed a liver CAD for automatic classification of Hepatocellular (malignant) and Hemangioma (benign) liver tumors from CT imaging using PNN classifier. Liver and tumors are segmented using region growing and alternative fuzzy c-means (AFCM) respectfully followed by feature extraction step using GLCM, wavelet coefficient texture (WCT) and contourlet coefficient texture (CCT). Probabilistic neural network (PNN) is used as a classifier for distinguishing malignant and benign liver tumors with an accuracy of 96.7%. Adcock et al. (2014) also proposed a comprehensive liver CAD system able to classify tumors based on histology (benign, malignant), density (hypodense, hyperdense) and type (cyst, Hemangioma, metastasis) using a CT dataset. Their proposed method based on multidimensional persistent homology, matching metric and a support vector machine SVM classifier was able to achieve an accuracy of 80.56%. Doron et al. (2014) proposed a liver CAD for automatic classification of tumors into benign and malignant from CT modality using an SVM classifier. Tumors are segmented manually followed by feature extraction step using GLCM, local binary patterns (LBP), gabor-based LBP (GLBP) and gray level intensities. The classification accuracy is reported as 97%. Alahmer and Ahmed (2015) proposed a liver CAD for automatic classification of tumors into benign and malignant from CT modality using an SVM classifier. Liver and tumors are segmented automatically followed by feature extraction step using GLCM and histogram analysis, the classification accuracy is reported as 97%.

### 9.1 Summary

Liver CAD systems are mostly developed based on discerning between healthy and pathological livers or between benign and malignant tumors. Furthermore, the majority of these CAD systems are based on manual segmentation of liver and liver tumors while those with automatic segmentation are usually built around simpler segmentation algorithms available with lower accuracies, especially in liver segmentation step. Thus, some of the most impor-

tant aspects of liver cancer treatment and planning are not included in these systems, such as selective internal radiation therapy planning and tumor burden analysis. With the integration of better liver and liver tumor segmentation, the capabilities of most of these systems can be expanded dramatically as these CAD systems would be able to provide much more functionalities given the proper input data.

Although the state of the art classifiers has been used in many of these CAD systems, their contribution in overall liver treatment planning can be considered minimal compared to more evolved CAD systems used in other medical tasks such as the breast cancer. An accurate computer-assisted detection/diagnosis system with precise segmentation of the liver and liver tumors can have a great effect in the overall treatment of the patient as accurate tumor volume and location estimation of all tumors in the liver can result in the planning of the best course of treatment. Table 5 represents some of the most accurate liver CAD systems developed for Liver using CT imaging modality.

## 10 Conclusions

In this paper, a review of CAD systems developed for liver treatment along with liver, liver tumor and vasculature segmentation methods are given. Several conclusions can be derived from previous works. First, methods relying solely on pixel intensity do not seem sufficient for lesion segmentation other than metastases. Then, liver lesion segmentation seems to be more accurate if done inside a liver envelope, in particular for automatic segmentation methods. Finally, machine learning techniques seem to considerably increase tumor detection and segmentation accuracy.

Basing a segmentation method solely on intensity is not efficient for tumor and vasculature segmentation. Although compared to healthy liver, some primary tumors and many metastases have distinct intensity ranges, these ranges vary based on imaging system and patient anatomy while many primary tumors could only be accurately identified based on their texture features. This is also evident in the literature as most approaches incorporating texture features and machine learning methods have the most accurate segmentation across different lesions. Machine learning can significantly increase the accuracy of liver tumor segmentation as the best methods use machine learning techniques. On the other hand, working inside a liver envelope yields better results in case of segmenting and classifying the lesions inside the liver, previous works have shown that segmentation of liver lesions was more accurate when done inside liver only, in particular for automatic methods.

Compared to recent automatic methods, semi-automatic methods do not offer any notable advantages. Some of the best results for liver tumor segmentation are indeed obtained by automatic methods. Moreover, an automatic segmentation offers two noticeable advantages compared to a semi-automatic method. First, automatic segmentation does not require any user interaction and is usually much faster compared to other segmentation methods and more importantly it does not require constant user input. Second, as there is no reliance on user interaction, the results are reproducible.

Although many liver segmentation methods have been proposed, there is still room for improvement especially in pathological livers where irregular liver shape and intensity patterns make automatic segmentation challenging. Furthermore, tumor and vasculature segmentation methods are even less developed and researched as these segmentations seem to suffer from a lack of appropriate and publicly accessible datasets. On the other hand, developed CAD systems for livers are amongst the least developed compared to some other

**Table 5** Comparison between some of the more accurate liver CAD methods published

| Method | Classifier | Features | Classification | Liver segmentation | Tumor segmentation | Accuracy | Dataset size |
|---|---|---|---|---|---|---|---|
| Gunasundari and Ananthi (2012) | PNN | GLCM FDCT | HCC and hemangioma tumors | Gray level and morphological | FCM | 96% | 70 slices |
| Kayaaltı et al. (2012) | SVM | DWT, GLCM, DFT | Seven different stages of liver fibrosis | Not required | Manual | 90% pairwise classification 37% in stage | 116 CT series |
| Kumar et al. (2013a) | PNN | GLCM WCT CCT | Malignant and benign tumors | Region growing | A-FCM | 96.7% | 300 slices |
| Adcock et al. (2014) | SVM | Matching metric | Histology (benign, malignant), density (hypodense, hyperdense) and type (cyst, Hemangioma, metastasis) | Not required | Manual | 80.56% | 132 tumors |
| Hameed and Kumar (2012) | PNN | GLCM | Malignant and benign tumors | Not required | Manual | 84% | Not mentioned |
| Hameed and Kumar (2012) | PCNN | GLCM | Malignant and benign tumors | Not required | Manual | 87% | Not mentioned |
| Duda et al. (2013) | AdaBoost | GLCM | Cholangiocarcinoma, cirrhotic, hepatocellular carcinoma tumors and healthy liver | Not required | Manual | 90% | 72 CT series |
| Mala and Sadasivam (2006) | LVQ-NN | WCT | Malignant and benign tumors | Not required | Manual | 92% | 100 slices |

**Table 5** continued

| Method | Classifier | Features | Classification | Liver segmentation | Tumor segmentation | Accuracy | Dataset size |
|---|---|---|---|---|---|---|---|
| Mala and Sadasivam (2010) | PNN | WCT | Fatty and cirrhotic liver | Not required | Manual | 95% | 100 slices |
| Doron et al. (2014) | SVM | GLCM LBP GLBP | Malignant and benign tumors | Not required | Manual | 97% | 92 tumors |
| Alahmer and Ahmed (2015) | SVM | GLCM and histogram analysis | Malignant and benign tumors | FCM | Region growing | 98.3% | 12 CT series |

medical CAD systems available, especially these CAD systems lack tumor burden analysis, SIRT calculation and other liver treatment related analysis. While most of these CAD systems utilize state of the art classification methods, they use either manual segmentation steps or are based on simple segmentation methods compared to other proposed segmentation methods. An accurate liver, liver tumor and liver blood vessel network segmentation can widen the capabilities of these CAD systems considerably.

## References


Abdel-massieh NH, Hadhoud MM, Amin KM (2010) Fully automatic liver tumor segmentation from abdominal CT scans. In: Computer engineering and systems (ICCES) international conference. IEEE, pp 197–202

Adcock A, Rubin D, Carlsson G (2014) Classification of hepatic tumors using the matching metric. Comput Vis Image Underst 121:36–42

Alahmer H, Ahmed A (2015) Computer-aided classification of liver tumors using contrasting features difference. In: ICMISC 2015 : 17th international conference on medical image and signal computing, pp 27–28

Albain KS, Swann RS, Rusch VW, Turrisi AT, Shepherd FA, Smith C, Chen Y, Livingston RB, Feins RH, Gandara DR, Fry WA (2009) Radiotherapy plus chemotherapy with or without surgical resection for stage III non-small-cell lung cancer: a phase III randomised controlled trial. Lancet 374:379–386

Al-Nahhas A, Szyszko T, Tait P, Damrah O, Canelo R (2006) Selective internal radiation therapy. In: Liver and biliary tract surgery. Springer, Vienna, pp 409–418

Al-Shaikhli SDS, Yang MY, Rosenhahn B (2015) Automatic 3D liver segmentation using sparse representation of global and local image information via level set formulation. arXiv preprint arXiv:1508.01521

Anter AM, Azar AT, Hassanien AE, El-Bendary N, ElSoud MA (2013) Automatic computer aided segmentation for liver and hepatic tumors using hybrid segmentations techniques. In: Computer science and information systems (FedCSIS), 2013 federated conference on, 2013. IEEE, pp 193–198

Anter AM, Hassanien AE, ElSoud MAA, Tolba MF (2014) Neutrosophic sets and fuzzy C-means clustering for improving CT liver image segmentation. In: Proceedings of the fifth international conference on innovations in bio-inspired computing and applications IBICA 2014. Springer, pp 193–203

Bauknecht HC, Romano VC, Rogalla P, Klingebiel R, Wolf C, Bornemann L, Hamm B, Hein PA (2010) Intra-and interobserver variability of linear and volumetric measurements of brain metastases using contrast-enhanced magnetic resonance imaging. Investig Radiol 45:49–56

Beck A, Aurich V (2007) HepaTux-a semiautomatic liver segmentation system 3D segmentation. In: Proceedings of 3D segmentation in the clinic: a grand challenge, pp 225–233

Beichel R, Pock T, Janko C, Zotter RB, Reitinger B, Bornik A, Palagyi K, Sorantin E, Werkgartner G, Bischof H, Sonka M (2004) Liver segment approximation in CT data for surgical resection planning. In: Proceedings of SPIE, vol 5370, pp 1435–1446

Beichel R, Bauer C, Bornik A, Sorantin E, Bischof H (2007) Liver segmentation in CT data: a segmentation refinement approach. In: Proceedings of 3D segmentation in the clinic: a grand challenge, pp 235–245

Ben Saïd T, Azaiz O, Chaieb F, M'hiri S, Ghorbel F (2010) Segmentation of liver tumor using HMRF-EM algorithm with Bootstrap resampling. In: Proceedings of the 5th international symposium on I/V communications and mobile network (ISVC), 2010. IEEE, pp 1–4

Ben-Dan I, Shenhav E (2008) Liver tumor segmentation in CT images using probabilistic methods. In: MICCAI Workshop, p 43

Bilello M, Gokturk SB, Desser T, Napel S, Jeffrey RB Jr, Beaulieu CF (2004) Automatic detection and classification of hypodense hepatic lesions on contrast-enhanced venous-phase CT. Med Phys 31(9):2584–2593

Bolte H, Jahnke T, Schäfer FK, Wenke R, Hoffmann B, Freitag-Wolf S, Dicken V, Kuhnigk JM, Lohmann J, Voss S, Knöß N (2007) Interobserver-variability of lung nodule volumetry considering different segmentation algorithms and observer training levels. Eur J Radiol 64:285–295

Bornemann L, Dicken V, Kuhnigk JM, Wormanns D, Shin HO, Bauknecht HC, Diehl V, Fabel M, Meier S, Kress O, Krass S (2007) OncoTREAT: a software assistant for cancer therapy monitoring. Int J Comput Assist Radiol Surg 1:231–242

Boykov Y, Veksler O, Zabih R (2001) Fast approximate energy minimization via graph cuts. IEEE Trans Pattern Anal Mach Intell 23:1222–1239

Camma C, Schepis F, Orlando A, Albanese M, Shahied L, Trevisani F, Andreone P, Craxì A, Cottone M (2002) Transarterial chemoembolization for unresectable hepatocellular carcinoma: meta-analysis of randomized controlled trials 1. Radiology 224:47–54

Campadelli P, Casiraghi E, Esposito A (2009) Liver segmentation from computed tomography scans: a survey and a new algorithm. Artif Intell Med 45:185–196

Casciaro S, Franchini R, Massoptier L, Casciaro E, Conversano F, Malvasi A, Lay-Ekuakille A (2012) Fully automatic segmentations of liver and hepatic tumors from 3-D computed tomography abdominal images: comparative evaluation of two automatic methods. IEEE Sens J 12(3):464–473

Caselles V, Kimmel R, Sapiro G (1997) Geodesic active contours. Int J Comput Vis 22:61–79

Chan TF, Vese L (2001) Active contours without edges. IEEE Trans Image Process 10:266–277

Chartrand G, Cresson T, Chav R, Gotra A, Tang A, DeGuise J (2014) Semi-automated liver CT segmentation using Laplacian meshes. In: Proceedings of the 11th international symposium on biomedical imaging (ISBI), 2014 IEEE, pp 641–644

Chen Y-W, Luo J, Dong C, Han X, Tateyama T, Furukawa A, Kanasaki S (2013) Computer-aided diagnosis and quantification of cirrhotic livers based on morphological analysis and machine learning. Comput Math Methods Med. doi:10.1155/2013/264809

Chi Y, Cashman PM, Bello F, Kitney A (2007) Discussion on the evaluation of a new automatic liver volume segmentation method for specified CT image datasets. In: Proceedings of 10th international conference on medical image computing and computer assisted intervention, pp 167–168

Chi Y, Liu J, Venkatesh SK, Huang S, Zhou J, Tian Q, Nowinski WL (2011) Segmentation of liver vasculature from contrast enhanced CT images using context-based voting. IEEE Trans Biomed Eng 58(8):2144–2153

Chi Y, Zhou J, Venkatesh SK, Huang S, Tian Q, Hennedige T, Liu J (2013) Computer-aided focal liver lesion detection. Int J Comput Assist Radiol Surg 8(4):511–525

Choudhary A, Moretto N, Ferrarese FP, Zamboni GA (2008) An entropy based multi-thresholding method for semi-automatic segmentation of liver tumors. In: MICCAI workshop, pp 43–94

Chung F, Delingette H (2013) Regional appearance modeling based on the clustering of intensity profiles. Comput Vis Image Underst 117:705–717

Ciecholewski M, Ogiela MR (2007) Automatic segmentation of single and multiple neoplastic hepatic tumors in CT images. In: Mira J, Álvarez JR (eds) Nature Inspired Problem-Solving Methods in Knowledge Engineering. IWINAC 2007. Lecture Notes in Computer Science, vol 4528. Springer, Heidelberg, pp 63–71

CIR dataset (2016) www.cancerimagingarchive.net. Accessed 1 Feb 2017

Cootes TF, Taylor CJ, Cooper DH, Graham J (1995) Active shape models-their training and application. Comput Vis Image Underst 61:38–59

Cover TM, Hart PE (1967) Nearest neighbor pattern classification. IEEE Trans Inf Theory 13:21–27

Dankerl P, Cavallaro A, Tsymbal A, Costa MJ, Suehling M, Janka R, Uder M, Hammon M (2013) A retrieval-based computer-aided diagnosis system for the characterization of liver tumors in ct scans. Acad Radiol 20:1526–1534

Doron Y, Mayer-Wolf N, Diamant I, Greenspan H (2014) Texture feature based liver tumor classification. In: SPIE medical imaging. International society for optics and photonics, p 90353K

Duda D, Krętowski M, Bézy-Wendling J (2013) Computer-aided diagnosis of liver tumors based on multi-image texture analysis of contrast-enhanced CT selection of the most appropriate texture features. Stud Log Gramm Rhetor 35:49–70

Erdt M, Steger S, Kirschner M, Wesarg S (2010) Fast automatic liver segmentation combining learned shape priors with observed shape deviation. In: Proceedings of the 23rd international symposium on computer-based medical systems (CBMS), 2010 IEEE, pp 249–254

Erdt M, Steger S, Sakas G (2012) Regmentation: a new view of image segmentation and registration. J Radiat Oncol Inform 4(1):1–23

Fabel M, von Tengg-Kobligk H, Giesel FL, Bornemann L, Dicken V, Kopp-Schneider A, Moser C, Delorme S, Kauczor HU (2011) Semi-automated volumetric analysis of lymph node metastases during follow-up—initial results. Eur Radiol 21:683–692

Falcão AX, Udupa JK, Samarasekera S, Sharma S, Hirsch BE, Lotufo RdA (1998) User-steered image segmentation paradigms: live wire and live lane. Graph Models Image Process 60:233–260

Fernández-de-Manuel L, Rubio JL, Ledesma-Carbayo MJ, Pascau J, Tellado JM, Ramón E, Desco M, Santos A (2009) 3D liver segmentation in preoperative CT images using a levelsets active surface method. In: Engineering in medicine and biology society. EMBC annual international conference of the IEEE, pp 3625–3628

Florin C, Paragios N, Funka-Lea G, Williams J (2007) Liver segmentation using sparse 3D prior models with optimal data support. In: Information processing in medical imaging. Springer, Heidelberg, pp 38–49

Foruzan AH, Zoroofi RA, Hori M, Sato Y (2009) Liver segmentation by intensity analysis and anatomical information in multi-slice CT images. Int J Comput Assist Radiol Surg 4:287–297
Freiman M, Eliassaf O, Taieb Y, Joskowicz L, Sosna J (2008) A bayesian approach for liver analysis: algorithm and validation study. In: Medical image computing and computer-assisted intervention-MICCAI 2008. Springer, pp 85–92
Freiman M, Cooper O, Lischinski D, Joskowicz L (2011) Liver tumors segmentation from CTA images using voxels classification and affinity constraint propagation. Int J Comput Assist Radiol Surg 6:247–255
Furukawa D, Shimizu A, Kobatake H (2007) Automatic liver segmentation method based on maximum a posterior probability estimation and level set method 3D Segmentation. In: Proceedings of 3D segmentation in the clinic: a grand challenge, pp 117–124
Gao L, Heath DG, Kuszyk BS, Fishman EK (1996) Automatic liver segmentation technique for three-dimensional visualization of CT data. Radiology 201:359–364
Garamendi JF, Malpica N, Martel J, Schiavi E (2007) Automatic segmentation of the liver in CT using level sets without edges. In: Pattern recognition and image analysis. Springer, pp 161–168
Gobbi PG, Broglia C, Di Giulio G, Mantelli M, Anselmo P, Merli F, Zinzani PL, Rossi G, Callea V, Iannitto E, Paulli M (2004) The clinical value of tumor burden at diagnosis in Hodgkin lymphoma. Cancer 101:1824–1834
Goryawala M, Gulec S, Bhatt R, McGoron AJ, Adjouadi M (2014) A low-interaction automatic 3D liver segmentation method using computed tomography for selective internal radiation therapy. BioMed Res Int 2014:198015. doi:10.1155/2014/198015
Grendell JH, Mcquaid KR, Friedman SL (1996) Current diagnosis and treatment in gastroenterology. In: Appleton and Lange
Gulec SA, Fong Y (2007) Yttrium 90 microsphere selective internal radiation treatment of hepatic colorectal metastases. Arch Surg 142(7):675–682
Gunasundari S, Ananthi MS (2012) Comparison and evaluation of methods for liver tumor classification from CT datasets. Int J Comput Appl 39:46–51
Habib A, Neuschwander-Tetri B, Friedman S, McQuaid K, Grendell J (2003) Current diagnosis and treatment in gastroenterology. McGraw Hill, Philadelphia
Häme Y (2008) Liver tumor segmentation using implicit surface evolution. Midas J 1–10
Hameed RS, Kumar S (2012) Assessment of neural network based classifiers to diagnose focal liver tumors using CT images. Proced Eng 38:4048–4056
Häme Y, Pollari M (2012) Semi-automatic liver tumor segmentation with hidden Markov measure field model and non-parametric distribution estimation. Med Image Anal 16:140–149
Hann LE, Winston CB, Brown KT, Akhurst T (2000) Diagnostic imaging approaches and relationship to hepatobiliary cancer staging and therapy. In: Seminars in surgical oncology, vol 2. Wiley, Hoboken, pp 94–115
Heckel F, Meine H, Moltz JH, Kuhnigk JM, Heverhagen JT, Kießling A, Buerke B, Hahn HK (2014) Segmentation-based partial volume correction for volume estimation of solid tumors in CT. IEEE T Image Process 33:462–480
Heimann T, Wolf I, Meinzer H-P (2006) Active shape models for a fully automated 3D segmentation of the liver: an evaluation on clinical data. In: Medical image computing and computer-assisted intervention–MICCAI 2006. Springer, pp 41–48
Heimann T, Meinzer H-P, Wolf I (2007a) A statistical deformable model for the segmentation of liver CT volumes. In: MICCAI 2007 Workshop Proceedings: 3D Segmentation in the clinic - a grand challenge, pp 161–166
Heimann T, Münzing S, Meinzer H-P, Wolf I (2007b) A shape-guided deformable model with evolutionary algorithm initialization for 3D soft tissue segmentation. In; Information processing in medical imaging. Springer, pp 1–12
Heimann T, Van Ginneken B, Styner MA, Arzhaeva Y, Aurich V, Bauer C, Beck A, Becker C, Beichel R, Bekes G, Bello F (2009) Comparison and evaluation of methods for liver segmentation from CT datasets. IEEE Trans Image Process 28:1251–1265
Heussel C, Meier S, Wittelsberger S, Götte H, Mildenberger P, Kauczor H (2007) Follow-up CT measurement of liver malignoma according to RECIST and WHO vs. volumetry. RoFo: Fortschr Geb Ront Nukl 179:958–964
Huang J, Meng L, Qu W, Wang C (2011) Based on statistical analysis and 3D region growing segmentation method of liver. In: Proceedings of the 3rd international conference on advanced computer control (ICACC), 2011. IEEE, pp 478–482
Huang W, Li N, Lin Z, Huang G, Zong W, Zhou J, Duan Y (2013) Liver tumor detection and segmentation using kernel-based extreme learning machine. In: Engineering in medicine and biology society (EMBC), 2013 35th annual international conference of the IEEE, 2013. IEEE, pp 3662–3665

Huang C, Li X, Jia F (2014a) Automatic liver segmentation using multiple prior knowledge models and free: form deformation. In: Proceedings of the VISCERAL challenge at ISBI, CEUR workshop proceedings, pp 22–24

Huang W, Yang Y, Lin Z, Huang G-B, Zhou J, Duan Y, Xiong W (2014b) Random feature subspace ensemble based extreme learning machine for liver tumor detection and segmentation. In: Engineering in medicine and biology society (EMBC), 2014 36th annual international conference of the IEEE. IEEE, pp 4675–4678

IRCAD dataset (2016) www.ircad.fr/research/3dircadb/. Accessed 1 Feb 2017

Jagannath S, Velasquez WS, Tucker SL, Fuller LM, McLaughlin PW, Manning JT, North LB, Cabanillas FC (1986) Tumor burden assessment and its implication for a prognostic model in advanced diffuse large-cell lymphoma. J Clin Oncol 4:859–865

Jimenez D, Fernandez-de-Manuel L, Pascau J, Tellado JM, Ramon E, Desco M, Santos A, Ledesma-Carbayo MJ (2011) Optimal multiresolution 3D level-set method for liver segmentation incorporating local curvature constraints. In: Engineering in medicine and biology society, EMBC, 2011 annual international conference of the IEEE, 2011. IEEE, pp 3419–3422

Jingran W, Xiaoyan Z, Ye X, Zuofeng L, Lei L (2009) Comparison of AdaBoost and logistic regression for detecting colorectal cancer patients with synchronous liver metastasis. In: International conference on biomedical and pharmaceutical engineering, 2009. ICBPE'09, pp 1–6

Jolly M, Grady L (2008) 3D general tumor segmentation in CT. In: Biomedical imaging: from nano to macro, 2008. ISBI 2008. 5th IEEE international symposium on, 2008. IEEE, pp 796–799

Kainmüller D, Lange T, Lamecker H (2007) Shape constrained automatic segmentation of the liver based on a heuristic intensity model. In: Proceedings of 3D segmentation in the clinic: a grand challenge, pp 109–116

Kawata Y, Niki N, Kumazaki T (1996) Feature extraction of convex surfaces on blood vessels using cone-beam CT images. In: International conference on image processing, vol. 3. IEEE, pp 315–318

Kayaaltı Ö et al. (2012) Staging of the liver fibrosis from CT images using texture features. In: Proceedings of the 7th international symposium on health informatics and bioinformatics (HIBIT), 2012. IEEE, pp 47–52

Kim PU, Jung Lee Y, Jung Y, Cho JH, Kim MN (2007) Liver extraction in the abdominal CT image by watershed segmentation algorithm. In: World congress on medical physics and biomedical engineering. Springer, pp 2563–2566

Kirbas C, Quek FK (2003) Vessel extraction techniques and algorithms: a survey. In: Bioinformatics and bioengineering, 2003. Proceedings. Third IEEE symposium on 2003 Mar 10, pp 238–245

Kubota T (2008) Efficient automated detection and segmentation of medium and large liver tumors: CAD approach. In: MICCAI workshop, 2008

Kuhnigk J-M, Dicken V, Bornemann L, Bakai A, Wormanns D, Krass S, Peitgen H-O (2006) Morphological segmentation and partial volume analysis for volumetry of solid pulmonary tumors in thoracic CT scans. IEEE Trans Image Process 25:417–434

Kumar S, Moni R, Rajeesh J (2013a) An automatic computer-aided diagnosis system for liver tumours on computed tomography images. Comput Electr Eng 39:1516–1526

Kumar S, Moni R, Rajeesh J (2013b) Automatic liver and tumor segmentation: a primary step in diagnosis of liver diseases. Signal Image Video Process 7:163–172

Lamecker H, Lange T, Seebass M (2004) Segmentation of the liver using a 3D statistical shape model. Konrad-Zuse-Zentrum für Informationstechnik, Berlin

Lee C, Chung C, Tsai M (2003) Identifying multiple abdominal organs from CT image series using a multi-module contextual neural network and spatial fuzzy rules. IEEE Trans Inf Technol Biomed 7:208–217

Lee J, Kim N, Lee H, Seo JB, Won HJ, Shin YM, Shin YG (2007) Efficient liver segmentation exploiting level-set speed images with 2.5 D shape propagation. In: 3D segmentation in the clinic: a grand challenge, pp 189–196

Leventon ME, Grimson WEL, Faugeras O (2000) Statistical shape influence in geodesic active contours. In: Computer vision and pattern recognition, 2000. Proceedings. IEEE conference on, 2000. IEEE, pp 316–323

Li K, Wu X, Chen DZ, Sonka M (2006a) Optimal surface segmentation in volumetric images-a graph-theoretic approach. IEEE Trans Pattern Anal 28:119–134

Li Y, Hara S, Shimura K (2006b) A machine learning approach for locating boundaries of liver tumors in CT images. In: Proceedings of the 18th international conference on pattern recognition, 2006. ICPR 2006. IEEE, pp 400–403

Li C, Wang X, Eberl S, Fulham M, Yin Y, Feng D (2010) Fully automated liver segmentation for low-and high-contrast CT volumes based on probabilistic atlases. In: Proceedings of the 17th IEEE international conference on image processing (ICIP), 2010. IEEE, pp 1733–1736

Li BN, Chui CK, Chang S, Ong SH (2011) Integrating spatial fuzzy clustering with level set methods for automated medical image segmentation. Comput Biol Med 41:1–10
Li C, Li A, Wang X, Feng D, Eberl S, Fulham M (2014a) A new statistical and Dirichlet integral framework applied to liver segmentation from volumetric CT images. In: 13th international conference on IEEE control automation robotics and vision (ICARCV), pp 642–647
Li D, Liu L, Chen J, Li H, Yin Y (2014b) A multistep liver segmentation strategy by combining level set based method with texture analysis for CT images. In: Proceedings of the 2014 IEEE international conference on orange technologies (ICOT). IEEE, pp 109–112
Li X, Huang C, Jia F, Li Z, Fang C, Fan Y (2014c) Automatic liver segmentation using statistical prior models and free-form deformation. In: Medical computer vision: algorithms for big data. Springer, pp 181–188
Liang P, Wang Y, Yu X, Dong B (2009) Malignant liver tumors: treatment with percutaneous microwave ablation—complications among cohort of 1136 patients 1. Radiology 251:933–940
Liao M, Zhao YQ, Wang W, Zeng YZ, Yang Q, Shih FY, Zou BJ (2016) Efficient liver segmentation in CT images based on graph cuts and bottleneck detection. Phys Med 32(11):1383–1396
Lim S, Jeong Y, Ho Y (2004) Automatic segmentation of the liver in CT images using the watershed algorithm based on morphological filtering. In: Medical imaging 2004. International society for optics and photonics, pp 1658–1666
Lim S, Jeong Y, Ho Y (2005) Segmentation of the liver using the deformable contour method on CT images. In: Advances in multimedia information processing-PCM 2005. Springer, pp 570–581
Lim S, Jeong Y, Ho Y (2006) Automatic liver segmentation for volume measurement in CT Images. J Vis Commun Image Represent 17:860–875
Linguraru MG, Li Z, Shah F, Summers RM (2009) Automated liver segmentation using a normalized probabilistic atlas. In: SPIE medical imaging, 2009. International society for optics and photonics, p 72622R-72622R-72628
Linguraru MG, Richbourg WJ, Liu J, Watt JM, Pamulapati V, Wang S, Summers RM (2012a) Tumor burden analysis on computed tomography by automated liver and tumor segmentation. IEEE Trans Image Process 31:1965–1976
Linguraru MG, Richbourg WJ, Watt JM, Pamulapati V, Summers RM (2012b) Liver and tumor segmentation and analysis from CT of diseased patients via a generic affine invariant shape parameterization and graph cuts. In: Abdominal imaging computational and clinical applications. Springer, pp 198–206
Ling H, Zhou SK, Zheng Y, Georgescu B, Suehling M, Comaniciu D (2008) Hierarchical, learning-based automatic liver segmentation. In: IEEE conference on computer vision and pattern recognition CVPR 2008. IEEE, pp 1–8
Liu F, Zhao B, Kijewski PK, Wang L, Schwartz LH (2005) Liver segmentation for CT images using GVF snake. Med Phys 32:3699–3706
Livraghi T, Giorgio A, Marin G, Salmi A, De Sio I, Bolondi L, Pompili M, Brunello F, Lazzaroni S, Torzilli G (1995) Hepatocellular carcinoma and cirrhosis in 746 patients: long-term results of percutaneous ethanol injection. Radiology 197:101–108
Lu F, Wu F, Hu P, Peng Z, Kong D (2016) Automatic 3D liver location and segmentation via convolutional neural network and graph cut. Int J Comput Assist Radiol Surg 7:1–2
Luo H, Lu Q, Acharya RS, Gaborski R (2000) Robust snake model. In: Computer vision and pattern recognition, 2000, vol 1. Proceedings. IEEE conference on 2000, pp 452–457
Maklad AS, Matsuhiro M, Suzuki H, Kawata Y, Niki N, Moriyama N, Utsunomiya T, Shimada M (2013) Blood vessel-based liver segmentation through the portal phase of a CT dataset. In: SPIE medical imaging, 2013. International society for optics and photonics, p 86700X-86700X-86707
Mala K, Sadasivam V (2006) Wavelet based texture analysis of liver tumor from computed tomography images for characterization using linear vector quantization neural network. In: Proceedings of the international conference on advanced computing and communication. ADCOM 2006. IEEE, pp 267–270
Mala K, Sadasivam V (2010) Classification of fatty and cirrhosis liver using wavelet-based statistical texture features and neural network classifier international. J Softw Inform 4:151–163
Malladi R, Sethian JA (1996) Level set and fast marching methods in image processing and computer vision. In: Proceedings of the international conference on image processing, 1996. Proceedings. 1996 Sep 16, vol 1, pp 489–492
Malladi R, Kimmel R, Adalsteinsson D, Sapiro G, Caselles V, Sethian JA (1996) A geometric approach to segmentation and analysis of 3D medical images. In: Proceedings of the workshop on mathematical methods in biomedical image analysis, 1996 Jun 21, pp 244–252
Marcan M, Pavliha D, Music M, Fuckan I, Magjarevic R, Miklavcic D (2014) Segmentation of hepatic vessels from MRI images for planning of electroporation-based treatments in the liver. Radiol Oncol 48(3):267–281

Massoptier L, Casciaro S (2007) Fully automatic liver segmentation through graph-cut technique. In: Proceedings of the 29th annual international conference of the IEEE engineering in medicine and biology society, 2007. EMBS 2007, pp 5243–5246
Massoptier L, Casciaro S (2008) A new fully automatic and robust algorithm for fast segmentation of liver tissue and tumors from CT scans. Eur Radiol 18:1658–1665
Masuda Y, Foruzan AH, Tateyama T, Chen YW (2010) Automatic liver tumor detection using EM/MPM algorithm and shape information. In: Software Engineering and Data Mining (SEDM), 2010. 2nd International Conference on 2010. IEEE, pp 692–695
Masuda Y, Tateyama T, Xiong W, Zhou J, Wakamiya M, Kanasaki S, Furukawa A, Chen YW (2011) Liver tumor detection in CT images by adaptive contrast enhancement and the EM/MPM algorithm. In: Proceedings of the 18th IEEE international conference on image processing (ICIP), 2011. IEEE, pp 1421–1424
McInerney T, Terzopoulos D (1996) Deformable models in medical image analysis: a survey. Med Image Anal 1:91–108
MIDAS dataset (2016) www.insight-journal.org/midas/collection/view/38. Accessed 1 Feb 2017
Militzer A Hager T, Jager F, Tietjen C, Hornegger J (2010) Automatic detection and segmentation of focal liver lesions in contrast enhanced CT images. In: Proceedings of the 20th international conference on pattern recognition (ICPR), 2010 Aug 23, pp 2524–2527
Moghbel M, Mashohor S, Mahmud R, Saripan MIB (2016a) Automatic liver segmentation on computed tomography using random walkers for treatment planning. EXCLI J 15:434–445
Moghbel M, Mashohor S, Mahmud R, Saripan MIB (2016b) Automatic liver tumor segmentation on computed tomography for patient treatment planning and monitoring. EXCLI J 15:500–517
Moltz JH, Bornemann L, Dicken V, Peitgen H (2008) Segmentation of liver metastases in CT scans by adaptive thresholding and morphological processing. In: MICCAI workshop, 2008, vol 43, p 195
Moltz JH, Bornemann L, Kuhnigk JM, Dicken V, Peitgen E, Meier S, Bolte H, Fabel M, Bauknecht HC, Hittinger M, Kießling A (2009) Advanced segmentation techniques for lung nodules, liver metastases, and enlarged lymph nodes in CT scans. IEEE J Sel Top Signal 3:122–134
Moltz JH, Braunewell S, Rühaak J, Heckel F, Barbieri S, Tautz L, Hahn HK, Peitgen HO (2011). Analysis of variability in manual liver tumor delineation in CT scans. In: Biomedical imaging: from nano to macro, 2011 IEEE international symposium on 2011 Mar 30, pp 1974–1977
Montagnat J, Delingette H (1997) Volumetric medical images segmentation using shape constrained deformable models. In: CVRMed-MRCAS'97, 1997. Springer, pp 13–22
Mortelé KJ, Cantisani V, Troisi R, de Hemptinne B, Silverman SG (2003) Preoperative liver donor evaluation: imaging and pitfalls. Liver Transplant 1:9
Mostafa A, Fouad A, Elfattah MA, Hassanien AE, Hefny H, Zhu SY, Schaefer G (2015) CT liver segmentation using artificial bee colony optimisation. Proced Comput Sci 60:1622–1630
Nordlinger B, Guiguet M, Vaillant JC, Balladur P, Boudjema K, Bachellier P, Jaeck D (1996) Surgical resection of colorectal carcinoma metastases to the liver: a prognostic scoring system to improve case selection, based on 1568 patients. Cancer 77:1254–1262
Nugroho HA, Ihtatho D, Nugroho H (2008) Contrast enhancement for liver tumor identification. In: MICCAI workshop, 2008, vol 43. p 201
Okada T, Shimada R, Hori M, Nakamoto M, Chen Y-W, Nakamura H, Sato Y (2008a) Automated segmentation of the liver from 3D CT images using probabilistic atlas and multilevel statistical shape model. Acad Radiol 15:1390–1403
Okada T, Yokota K, Hori M, Nakamoto M, Nakamura H, Sato Y (2008b) Construction of hierarchical multi-organ statistical atlases and their application to multi-organ segmentation from CT images. In: Medical image computing and computer-assisted intervention-MICCAI 2008. Springer, New York, pp 502–509
Osher S, Fedkiw R (2006) Level set methods and dynamic implicit surfaces, vol 153. Springer, New York
Pamulapati V, Venkatesan A, Wood BJ, Linguraru MG (2011) Liver segmental anatomy and analysis from vessel and tumor segmentation via optimized graph cuts. In: International MICCAI workshop on computational and clinical challenges in abdominal imaging 2011 Sep 18. Springer, Berlin, pp 189–197
Pan S, Dawant BM (2001) Automatic 3D segmentation of the liver from abdominal CT images: a level-set approach. Int Soc Opt Photonics Med Imaging 2001:128–138
Park H, Bland PH, Meyer CR (2003) Construction of an abdominal probabilistic atlas and its application in segmentation. IEEE Trans Med Imaging 22:483–492
Park S, Seo K, Park J (2005) Automatic hepatic tumor segmentation using statistical optimal threshold. In: Computational science—ICCS 2005. Springer, pp 934–940
Platero C, Tobar MC, Sanguino J, Poncela JM, Velasco O (2011) Level set segmentation with shape and appearance models using affine moment descriptors. In: Pattern recognition and image analysis. Springer, pp 109–116

Pohle R, Toennies KD (2001) Segmentation of medical images using adaptive region growing. In: Medical imaging 2001. International society for optics and photonics, pp 1337–1346

Prasad SR, Jhaveri KS, Saini S, Hahn PF, Halpern EF, Sumner JE (2002) CT tumor measurement for therapeutic response assessment: comparison of unidimensional, bidimensional, and volumetric techniques-initial observations 1. Radiology 225:416–419

Puesken M, Buerke B, Gerss J, Frisch B, Beyer F, Weckesser M, Seifarth H, Heindel W, Wessling J (2010) Prediction of lymph node manifestations in malignant lymphoma: significant role of volumetric compared with established metric lymph node analysis in multislice computed tomography. J Comput Assist Tomogr 34:564–569

Qi Y, Xiong W, Leow WK, Tian Q, Zhou J, Liu J, Han T, Venkatesh SK, Wang SC (2008) Semi-automatic segmentation of liver tumors from CT scans using Bayesian rule-based 3D region growing. In: MICCAI workshop, 2008, vol 43. p 201

Rossi S, Di Stasi M, Buscarini E, Cavanna L, Quaretti P, Squassante E, Garbagnati F, Buscarini L (1994) Percutaneous radiofrequency interstitial thermal ablation in the treatment of small hepatocellular carcinoma. Cancer J Sci Am 1:73–81

Rossi S, Di Stasi M, Buscarini E, Quaretti P, Garbagnati F, Squassante L, Paties CT, Silverman DE, Buscarini L (1996) Percutaneous RF interstitial thermal ablation in the treatment of hepatic cancer. AJR Am J Roentgenol 167:759–768

Rusko L, Bekes G, Nemeth G, Fidrich M (2007) Fully automatic liver segmentation for contrast-enhanced CT images. In: Proceedings of 3D segmentation in the clinic: a grand challenge

Rusko L, Bekes G, Fidrich M (2009) Automatic segmentation of the liver from multi-and single-phase contrast-enhanced CT images. Med Image Anal 13:871–882

Rusko L, Perényi Á (2014) Automated liver lesion detection in CT images based on multi-level geometric features. Int J Comput Assist Radiol Surg 9(4):577–593

Saddi KA, Rousson M, Chefd'hotel C, Cheriet F (2007) Global-to-local shape matching for liver segmentation in CT imaging. In: Proceedings of MICCAI workshop on 3D segmentation in the clinic: a grand challenge, 2007, pp 207–214

Safdari M, Pasari R, Rubin D, Greenspan H (2013) Image patch-based method for automated classification and detection of focal liver lesions on CT. In: SPIE medical imaging 2013 Mar 18. International Society for Optics and Photonics, pp 86700Y–86700Y

Saito A, Yamamoto S, Nawano S, Shimizu A (2016) Automated liver segmentation from a postmortem CT scan based on a statistical shape model. Int J Comput Assist Radiol Surg 22:1–7

Saxena S, Sharma N, Sharma S, Singh SK, Verma A (2016) An automated system for atlas based multiple organ segmentation of abdominal CT images. BJMCS 12:1–4

Schenk A, Prause G, Peitgen H (2000) Efficient semiautomatic segmentation of 3D objects in medical images. In: Medical image computing and computer-assisted intervention—MICCAI 2000. Springer, pp 186–195

Schmidt G, Athelogou M, Schoenmeyer R, Korn R, Binnig G (2007) Cognition network technology for a fully automated 3D segmentation of liver. In: Proceedings of MICCAI workshop on 3D segmentation in the clinic: a grand challenge, 2007, pp 125–133

Schmidt G, Binnig G, Kietzmann M, Kim J (2008) Cognition network technology for a fully automated 3D segmentation of liver tumors. In: Proceedings of the miccai workshop—grand challenge liver tumor segmentation, 2008

Schwier M, Moltz JH, Peitgen H-O (2011) Object-based analysis of CT images for automatic detection and segmentation of hypodense liver lesions. Int J Comput Assist Radiol Surg 6(6):737–747

Seghers D, Slagmolen P, Lambelin Y, Hermans J, Loeckx D, Maes F, Suetens P (2007) Landmark based liver segmentation using local shape and local intensity models. In: Proceedings of the workshop of the 10th international conference on MICCAI, workshop on 3D segmentation in the clinic: a grand challenge, 2007, pp 135–142

Selle D, Preim B, Schenk A, Peitgen H-O (2002) Analysis of vasculature for liver surgical planning. IEEE Trans Med Imaging 21(11):1344–1357

Seo K, Park J (2005) Improved automatic liver segmentation of a contrast enhanced CT image. In: Advances in multimedia information processing, PCM 2005. Springer, pp 899–909

Sharma P, Malik S, Sehgal S, Pruthi J (2013) Computer aided diagnosis based on medical image processing and artificial intelligence methods. Int J Inf Comput Technol 3(9):887–892 (ISSN:0974-2239)

Shi C, Cheng Y, Liu F, Wang Y, Bai J, Tamura S (2015) A hierarchical local region-based sparse shape composition for liver segmentation in CT scans. Pattern Recognit 50:88–106

Shimizu A, Narihira T, Furukawa D, Kobatake H, Nawano S, Shinozaki K (2008a) Ensemble segmentation using AdaBoost with application to liver lesion extraction from a CT volume. Paper presented at the Proceedings of the MICCAI workshop on 3D segmentation in the clinic: a grand challenge II

Shimizu A, Narihira T, Furukawa D, Kobatake H, Nawano S, Shinozaki K (2008b) Ensemble segmentation using AdaBoost with application to liver tumor extraction from a CT volume. In: Proceedings of the MICCAI workshop on 3D segmentation in the clinic: a grand challenge II, 2008

Shimizu A, Nakagomi K, Narihira T, Kobatake H, Nawano S, Shinozaki K, Ishizu K, Togashi K (2010) Automated segmentation of 3D CT images based on statistical atlas and graph cuts. In: Medical computer vision. Recognition techniques and applications in medical imaging. Springer, pp 214–223

Slagmolen P, Elen A, Seghers D, Loeckx D, Maes F, Haustermans K (2007) Atlas based liver segmentation using nonrigid registration with a B-spline transformation model. In: Proceedings of 3D segmentation in the clinic: a grand challenge, 2007. pp 197–206

Sliver07 dataset (2016) www.Sliver07.org/. Accessed 1 Feb 2017

Smeets D, Stijnen B, Loeckx D, De Dobbelaer B, Suetens P (2008) Segmentation of liver metastases using a level set method with spiral-scanning technique and supervised fuzzy pixel classification. In: MICCAI workshop, 2008, p 43

Soler L, Delingette H, Malandain G, Montagnat J, Ayache N, Koehl C, Dourthe O, Malassagne B, Smith M, Mutter D, Marescaux J (2001) Fully automatic anatomical, pathological, and functional segmentation from CT scans for hepatic surgery. Comput Aided Surg 6:131–142

Song Y, Bulpitt AJ, Brodlie KW (2009) Liver segmentation using automatically defined patient specific B-spline surface models. In: Medical image computing and computer-assisted intervention—MICCAI 2009. Springer, pp 43–50

Song H, Zhang Q, Wang S (2014) Liver segmentation based on SKFCM and improved GrowCut for CT images. In: Proceedings of the 2014 IEEE international conference on bioinformatics and biomedicine (BIBM), 2014. IEEE, pp 331–334

Sonka M, Fitzpatrick JM (2000) Handbook of medical imaging (Vol 2, Medical image processing and analysis)

Stawiaski J, Decenciere E, Bidault F (2008) Interactive liver tumor segmentation using graph-cuts and watershed. In: Workshop on 3D segmentation in the clinic: a grand challenge II. Liver tumor segmentation challenge. MICCAI, New York, 2008

Susomboon R, Raicu DS, Furst J (2007) A hybrid approach for liver segmentation. In: Proceedings of MICCAI workshop on 3D segmentation in the clinic: a grand challenge, 2007. pp 151–160

Suzuki K, Kohlbrenner R, Epstein ML, Obajuluwa AM, Xu J, Hori M (2010) Computer-aided measurement of liver volumes in CT by means of geodesic active contour segmentation coupled with level-set algorithms. Med Phys 37:2159–2166

Taha AA, Hanbury A (2015) Metrics for evaluating 3D medical image segmentation: analysis, selection, and tool. BMC Med Imaging 15(1):29

Taieb Y, Eliassaf O, Freiman M, Joskowicz L, Sosna J (2008) An iterative bayesian approach for liver analysis: tumors validation study. In: MICCAI workshop, 2008. p 43

Tajima T, Zhang X, Kitagawa T, Kanematsu M, Zhou X, Hara T, Fujita H, Yokoyama R, Kondo H, Hoshi H, Nawano S (2007) Computer-aided detection (CAD) of hepatocellular carcinoma on multiphase CT images. In: Medical imaging 2007 Mar 8. International Society for Optics and Photonics, pp 65142Q–65142Q

Thakre AK, Dhenge AI (2013) CT liver image diagnosis classification system. Int J Adv Res Comput Commun Eng 2:891–894

Toledo R, Orriols X, Radeva P, Binefa X, Vitria J, Canero C, Villanuev JJ (2000) Eigensnakes for vessel segmentation in angiography. In: Proceedings of the 15th international conference on pattern recognition, 2000, vol 4. pp 340–343

Tomoshige S, Oost E, Shimizu A, Watanabe H, Nawano S (2014) A conditional statistical shape model with integrated error estimation of the conditions; application to liver segmentation in non-contrast CT images. Med Image Anal 18:130–143

Tozaki T, Kawata Y, Niki N, Ohmatsu H, Moriyama N (1995) 3-D visualization of blood vessels and tumor using thin slice CT images. In: Nuclear science symposium and medical imaging conference, 1994. IEEE Conference Record 1995, vol 3. pp 1470–1474

Tsai D, Tanahashi N (1994) Neural-network-based boundary detection of liver structure in ct images for 3-D visualization. In: Proceedings of the IEEE international conference on neural networks, 1994. IEEE world congress on computational intelligence, 1994. IEEE, pp 3484–3489

Tsai A, Yezzi A, Wells W, Tempany C, Tucker D, Fan A, Grimson WE, Willsky A (2003) A shape-based approach to the segmentation of medical imagery using level sets. IEEE Trans Med Imaging 22:137–154

Van Ginneken B, Frangi AF, Staal JJ, Romeny BM, Viergever MA (2002) Active shape model segmentation with optimal features. IEEE Trans Med Imaging 21:924–933

Van Rikoort E, Arzhaeva Y, van Ginneken B (2007) Automatic segmentation of the liver in computed tomography scans with voxel classification and atlas matching. In: Proceedings of the MICCAI Workshop 2007, pp 101–108

Vincey J (2013) Computer aided diagnosis for liver cancer feature extraction. Int J Eng Sci 11:27–30
Vorontsov E, Abi-Jaoudeh N, Kadoury S (2014) Metastatic liver tumor segmentation using texture-based omni-directional deformable surface models. In: Abdominal imaging. Computational and clinical applications. Springer, pp 74–83
Wang G, Zhang S, Xie H, Metaxas DN, Gu L (2015a) A homotopy-based sparse representation for fast and accurate shape prior modeling in liver surgical planning. Med Image Anal 19:176–186
Wang X, Yang J, Ai D, Zheng Y, Tang S, Wang Y (2015b) Adaptive mesh expansion model (AMEM) for liver segmentation from CT image. PLoS ONE 10:e0118064
Wang J, Cheng Y, Guo C, Wang Y, Tamura S (2016) Shape-intensity prior level set combining probabilistic atlas and probability map constrains for automatic liver segmentation from abdominal CT images. Int J Comput Assist Radiol Surg 11(5):817–826
Wimmer A, Soza G, Hornegger J (2007) Two-stage semi-automatic organ segmentation framework using radial basis functions and level sets 3D Segmentation. In: Proceedings of 3D segmentation in the clinic: a grand challenge, pp 179–188
Wimmer A, Hornegger J, Soza G (2008) Implicit active shape model employing boundary classifier. In: Proceedings of the 19th international conference on pattern recognition, 2008. ICPR 2008. IEEE, pp 1–4
Wimmer A, Soza G, Hornegger J (2009) A generic probabilistic active shape model for organ segmentation. In: Medical image computing and computer-assisted intervention—MICCAI 2009. Springer, pp 26–33
Wong D, Liu J, Fengshou Y, Tian Q, Xiong W, Zhou J, Qi Y, Han T, Venkatesh S, Wang SC (2008) A semi-automated method for liver tumor segmentation based on 2D region growing with knowledge-based constraints. In: MICCAI workshop, 2008, vol 43. p 159
Wu X, Spencer SA, Shen S, Fiveash JB, Duan J, Brezovich IA (2009) Development of an accelerated GVF semi-automatic contouring algorithm for radiotherapy treatment planning. Comput Biol Med 39:650–656
Wu D, Liu D, Suehling M, Tietjen C, Soza G, Zhou KS (2012) Automatic detection of liver lesion from 3d computed tomography images. In: Computer Vision and Pattern Recognition Workshops (CVPRW), 2012. IEEE Computer Society Conference on 2012. IEEE, pp 31–37
Wu W, Zhou Z, Wu S, Zhang Y (2016) Automatic liver segmentation on volumetric CT images using supervoxel-based graph cuts. Comput Math Methods Med 5:2016
Xu C, Prince JL (1998) Snakes, shapes, and gradient vector flow. IEEE Trans Med Imaging 7:359–369
Xu J, Suzuki K (2011) Computer-aided detection of hepatocellular carcinoma in hepatic CT: false positive reduction with feature selection. In: Proceedings of the 2011 IEEE international symposium on biomedical imaging: from nano to macro, 2011. IEEE, pp 1097–1100
Xu Z, Burke RP, Lee CP, Baucom RB, Poulose BK, Abramson RG, Landman BA (2015) Efficient multi-atlas abdominal segmentation on clinically acquired CT with SIMPLE context learning. Med Image Anal 31:18–27
Yamada R, Sato M, Kawabata M, Nakatsuka H, Nakamura K, Takashima S (1983) Hepatic artery embolization in 120 patients with unresectable hepatoma. Radiology 148:397–401
Yi X, Zhong L, Lin J (2010) Liver ct image segmentation by local entropy method. In: Proceedings of the 2010 international conference on computer application and system modeling (ICCASM), 2010. IEEE, pp V11-591–V511-594
Zhang X, Tian J, Deng K, Wu Y, Li X (2010) Automatic liver segmentation using a statistical shape model with optimal surface detection. IEEE Trans Bio-Med Eng 57:2622
Zhang X, Tian J, Xiang D, Li X, Deng K (2011) Interactive liver tumor segmentation from ct scans using support vector classification with watershed. In: Engineering in medicine and biology society, EMBC, 2011 annual international conference of the IEEE, 2011. IEEE, pp 6005–6008
Zheng Y, Barbu A, Georgescu B, Scheuering M, Comaniciu D (2007) Fast automatic heart chamber segmentation from 3D CT data using marginal space learning and steerable features. In: Proceedings of the IEEE 11th international conference on computer vision, 2007. ICCV 2007. IEEE, pp 1–8
Zhou X, Kitagawa T, Hara T, Fujita H, Zhang X, Yokoyama R, Kondo H, Kanematsu M, Hoshi H (2006) Constructing a probabilistic model for automated liver region segmentation using non-contrast X-ray torso CT images. In: Medical image computing and computer-assisted intervention—MICCAI 2006. Springer, pp 856–863
Zhou J, Xiong W, Tian Q, Qi Y, Liu J, Leow WK, Han T, Venkatesh SK, Wang SC (2008) Semi-automatic segmentation of 3D liver tumors from CT scans using voxel classification and propagational learning. In: MICCAI workshop, 2008. p 43
Zhou JY, Wong DW, Ding F, Venkatesh SK, Tian Q, Qi YY, Xiong W, Liu JJ, Leow WK (2010) Liver tumour segmentation using contrast-enhanced multi-detector CT data: performance benchmarking of three semiautomated methods. Eur Radiol 20:1738–1748